(2)

AD

Reports Control Symbol
OSD - 1366

ASL TR-0314

THE SENSITIVITY OF THE RECEIVER COHERENCE DIAMETER AND MODULATION TRANSFER FUNCTION TO VARIATIONS OF A DAMP UNSTABLE ATMOSPHERE

July 1992

Henry Rachele
Arnold Tunick

US ARMY
LABORATORY COMMAND
ATMOSPHERIC SCIENCES LABORATORY
White Sands Missile Range, NM 88002-5501

NOTICES

Disclaimers

The findings in this report are not to be construed as an official Department of the Army position, unless so designated by other authorized documents.

The citation of trade names and names of manufacturers in this report is not to be construed as official Government indorsement or approval of commercial products or services referenced herein.

Destruction Notice

When this document is no longer needed, destroy it by any method that will prevent disclosure of its contents or reconstruction of the document.

REPORT DOCUMENTATION PAGE

Form Approved
OMB No. 0704-0188

1. AGENCY USE ONLY *(Leave blank)*

2. REPORT DATE
July 1992

3. REPORT TYPE AND DATES COVERED
Final

4. TITLE AND SUBTITLE
THE SENSITIVITY OF THE RECEIVER COHERENCE DIAMETER AND MODULATION TRANSFER FUNCTION TO VARIATIONS OF A DAMP UNSTABLE ATMOSPHERE

5. FUNDING NUMBERS
B-53A-B
611102.53A40.11

6. AUTHOR(S)
Henry Rachele and Arnold Tunick

7. PERFORMING ORGANIZATION NAME(S) AND ADDRESS(ES)
U.S. Army Atmospheric Sciences Laboratory
White Sands Missile Range, NM 88002-5501

8. PERFORMING ORGANIZATION REPORT NUMBER
ASL-TR-0314

9. SPONSORING/MONITORING AGENCY NAME(S) AND ADDRESS(ES)
U.S. Army Laboratory Command
Adelphi, MD 20783-1145

10. SPONSORING/MONITORING AGENCY REPORT NUMBER

11. SUPPLEMENTARY NOTES

12a. DISTRIBUTION/AVAILABILITY STATEMENT
Approved for public release; distribution unlimited.

12b. DISTRIBUTION CODE

13. ABSTRACT *(Maximum 200 words)*

The purpose of this study was to examine the sensitivity of the receiver coherence diameter, r_o, and the modulation transfer function (MTF) to variations of the natural atmosphere from an assumed ideal average state and from misrepresentation of the atmospheric effects due to errors in measurement and processing of the basic meteorological parameters. The concept was simplified by assuming that all natural variations and errors due to sensor performance and positioning can be lumped and that they collectively are normally distributed, even though the natural variations are known not to be normal. For this study, the authors selected two sets of data to analyze. The data from Davis, California, were collected during unstable conditions with clear skies. Bar graphs were used to show distributions resulting from total errors. They include the friction velocity u*; windspeed V_r; temperature scaling parameter T*; specific humidity scaling parameter q*; Obukhov scaling length L; structure parameter C_n^2; and receiver coherence diameter r_o. Additionally, the authors take the minimum, maximum, and mean r_o for each case and plot the resulting near- and far-field slow MTF.

14. SUBJECT TERMS
optics, receiver coherence diameter, optical turbulence, modulation transfer functions

15. NUMBER OF PAGES
37

16. PRICE CODE

17. SECURITY CLASSIFICATION OF REPORT	18. SECURITY CLASSIFICATION OF THIS PAGE	19. SECURITY CLASSIFICATION OF ABSTRACT	20. LIMITATION OF ABSTRACT
Unclassified	Unclassified	Unclassified	SAR

NSN 7540-01-280-5500

Standard Form 298 (Rev. 2-89)
Prescribed by ANSI Std. Z39-18
298-102

CONTENTS

LIST OF ILLUSTRATIONS 4

1. INTRODUCTION 5

2. EQUATIONS 6

3. RECEIVER COHERENCE DIAMETER (r_o) 20

4. THE MODULATION TRANSFER FUNCTION 20

5. EXAMPLES 21

6. RESULTS 22

7. SUMMARY AND CONCLUSIONS 23

LITERATURE CITED 39

DISTRIBUTION LIST 41

LIST OF ILLUSTRATIONS

Table

1. Micrometeorological Parameters from the Davis, CA, Data 21

Figures

1. Case 1 - Random distribution for: (a) u* and (b) normal distribution for V_r 24

2. Case 1 - Random distribution for: (a) T*, (b) q*, and (c) L 26

3. Case 1 - Distribution for C_n^2: (a) random and (b) probability.......... 28

4. Case 1 - (a) Random distribution for r_o and (b) the resultant MTF for a slant path looking upward 29

5. Case 1 - (a) Random distribution for r_o and (b) the resultant MTF for a slant path looking downward 30

6. Case 2 - Random distribution for: (a) u* and (d) normal distribution for V_r 31

7. Case 2 - Random distribution for: (a) T*, (b) q*, and (c) L 33

8. Case 2 - Distribution for C_n^2: (a) random and (b) probability.......... 35

9. Case 1 - (a) Random distribution for r_o and (b) the resultant MTF for a slant path looking upward 36

10. Case 1 - (a) Random distribution for r_o and (b) the resultant MTF for a slant path looking downward 37

1. INTRODUCTION

This technical report is a brief, but significant, extension of an earlier report Rachele and Tunick (1992) in which the focus of the study was to determine the sensitivity of the optical parameter C_n^2 due to variations of the observed atmosphere from a true (ideal) average state. Estimates of C_n^2 are strongly dependent on the vertical gradient of the real index of refraction, which, in turn, is very sensitive to the vertical gradients of temperature and moisture. Variations of the atmosphere from the true average state, which we characterize by Monin-Obukhov similarity equations, were envisioned to be due to sensor response errors, sensor misplacement, and data processing (resulting in incorrect values of atmospheric temperature, pressure, relative humidity, and wind) and natural variations of the atmosphere due to naturally uneven terrain and nonsteady state and nonhomogeneous conditions. We simplified our concept by assuming that all natural variations and errors due to sensor performance and positioning could be lumped, and that collectively they are normally distributed, even though the natural variations are known not to be normal (Pries and Appleby, 1967; Izumi 1971).

The purpose of this study was to approximate variations in the receiver coherence diameters and modulation transfer function (MTF) due to variations in C_n^2. Many of the formulations and results presented in this report were also used in the earlier report (Rachele and Tunick, 1992).

We alert the reader to a possible pitfall of misinterpretation and application. The so-called natural variations used in this study were not determined from field data, instead they are creations on our part of what we felt were reasonable. In particular, we not only required that the distributions of the fluctuations be normally distributed, but we also specified the values of the variances. (As such, the results are at best representations of C_n^2, r_o, and MTF to the input parameters, as specified, and should not be interpreted as real-world results.) The mean values, however, were determined from field data (Stenmark and Drury, 1970).

Critical to this study is the understanding that we deal with long-term (30 min) mean values and departures from the long-term means. Ideally, we assume that the atmosphere is in steady state and horizontally homogeneous. We recognize, however, for various reasons it is not. We attempt to observe (measure) and model the atmosphere in this ideal framework, but allow for adjustments by randomizing the basic inputs to the model. If indeed the ideal were possible, then the long- and short-term mean values that we use would be precise and representative of the atmosphere. We know, however, that this picture is unrealistic to one degree or another. Our concern then is to determine the combined effect of the natural variations and sensor errors on the character of the atmosphere and subsequently effects on the parameters of interest.

The types and numbers of atmospheric measurements needed to characterize the atmosphere vary with the models used and with the researchers preferences and budget. In this study, we assumed that measurements of temperature, pressure, windspeed, and relative humidity are made at two levels in the lower atmosphere. Each of these basic measurements is averaged over a finite time period, 30 min. We will not, in this report, discuss the sensors, their response characteristics,

etc., or the methods for recording or processing the data. Instead, we assume that the long-term (30 min) values, however determined, can be in "error." We also assume that the sensors may not be precisely positioned with height. In what follows, we present a methodology, including formulations, for estimating the sensitivity of C_n^2, r_o, and MTF due to the natural variations and to sensor errors.

2. EQUATIONS

In this section, we present the basic expression for C_n^2 based on Tatarski (1961), which is strongly dependent on the vertical gradient of the real index of refraction $\frac{dn}{dz}$. Moreover, $\frac{dn}{dz}$ has been shown to be a function of the vertical gradient of potential temperature, $\frac{d\theta}{dz}$, and specific humidity, $\frac{dq}{dz}$. If one assumes, as we do, that the atmosphere is in steady state and horizontally homogeneous, then $\frac{d\theta}{dz}$ and $\frac{dq}{dz}$ and consequently $\frac{dn}{dz}$ can be replaced by their partial derivatives, $\frac{\partial\theta}{\partial z}$, $\frac{\partial q}{\partial z}$, and $\frac{\partial n}{\partial z}$. In our approach we represent $\frac{\partial\theta}{\partial z}$ and $\frac{\partial q}{\partial z}$ and the wind gradient $\frac{\partial v}{\partial z}$ by "similarity" expressions given in equations (2) through (4). Observation of these equations shows that these gradients are primarily functions of height Z, u^*, θ^*, q^* *and* L, and hence the gradients are a function of the variations of these quantities. We then proceed to show how one can formulate variations in u^*, θ^*, q^*, and L, that is, du^*, $d\theta^*$, dq^*, and dL, as a function of variations in V, P, T, Z, and f at two heights.

Next we show that the basic form of C_n^2 can be recast in terms of θ^* *and* q^*, equation (65). Hence, if θ^* *and* q^* are allowed to vary in a random way, we can compute variations of C_n^2.

The basic formulation we use for computing C_n^2 is based on Tatarski (1961); that is,

$$C_n^2 = b\left(\frac{K_H}{\epsilon^{1/3}}\right)\left(\frac{dn}{dz}\right)^2 \quad , \tag{1}$$

where

b = a constant = 3.2 (Wyngaard, 1973; Hill, 1989; Andreas, 1988)

$K_H = \frac{u^* k z}{\Phi_H}$ = turbulent exchange coefficient for heat

u^* - friction velocity

k - von Karman's constant (0.4)

z - height above ground

$\phi_H = \left(1 - 15\frac{z}{L}\right)^{1/2}$ = dimensionless lapse rate for heat in unstable conditions.

$\epsilon = \left(\phi_M - \frac{z}{L}\right)\frac{u^{*3}}{kz}$ = energy dissipation rate, Panofsky (1968)

$\phi_M = \left(1 - 15\frac{z}{L}\right)^{-1/4}$ = dimensionless lapse rate for momentum

L - Obukhov (1946) length

n - real index of refraction

$\frac{dn}{dz}$ - height derivative of n

In addition, $\frac{dn}{dz}$ is written as a function of the height derivatives of potential temperature and specific humidity, that is, $\frac{d\theta}{dz}$ and $\frac{dq}{dz}$ (Tunick and Rachele, 1991). One way of evaluating $\frac{d\theta}{dz}$ and $\frac{dq}{dz}$ is to assume that they are expressible in similarity form, which implies that we are considering mean values. In particular, for unstable atmospheric conditions, we write

$$\frac{\partial\theta}{\partial z} = \frac{\theta^*}{kz}\left(1 - 15\frac{z}{L}\right)^{-1/2} \tag{2}$$

$$\frac{\partial q}{\partial z} = \frac{q^*}{kz}\left(1 - 15\frac{z}{L}\right)^{-1/2} \tag{3}$$

$$\frac{\partial v}{\partial z} = \frac{u^*}{kz}\left(1 - 15\frac{z}{L}\right)^{-1/4} , \tag{4}$$

where

q - specific humidity

v - windspeed

θ^* - temperature scaling length

q^* - specific humidity scaling length

u^* - friction velocity

$$L = \frac{u*^2 \ T_{vr}}{kg \ \theta_v^*} , \tag{5}$$

where

g - acceleration due to gravity

T_r - temperature at a reference height Z_r

T_{vr} - virtual temperature at reference height - T_r $(1 + 0.61q_r)$ (6)

$$\theta_v^* = \theta^* + 0.61\theta_r q^* \ . \tag{7}$$

Note that to use equations (2) and (3) to approximate $\frac{d\theta}{dz}$ and $\frac{dq}{dz}$, we have imposed the conditions of steady state and horizontal homogeneity on the atmosphere. Furthermore, the similarity expression only makes sense in terms of mean values, which, for unstable conditions, involves time averages on the order of 30 min.

As mentioned earlier, the minimum amount of data we require to evaluate equations (2) through (4) are measurements of temperature, pressure, windspeed, and relative humidity at two heights. These data are then averaged over the total time interval.

Also, as stated previouslv, we assume that there are errors in the fidelity of measurement, the placement of the sensors, and the techniques for processing the data, resulting in errors in the estimates of the mean values. These errors are compounded by the natural transients that ampl'.fy the sensor errors. To quantify the effects of these errors (variations) on C_n^2, we first integrate equations (2) through (4), resulting in

$$\theta_2 = \theta_1 + \frac{\theta^*}{k} \left\{ \ln\left(\frac{y-1}{y+1}\right)\right\} \Big|_{y_2}^{y_1} \tag{8}$$

$$q_2 = q_1 + \frac{q^*}{k} \left\{ \ln\left(\frac{y'-1}{y'+1}\right)\right\} \Big|_{y_1'}^{y_2'} \tag{9}$$

$$v_2 = v_1 + \frac{u^*}{k} \left\{ \ln\left(\frac{x - 1}{x + 1}\right) + 2 \tan^{-1} x \right\} \Big|_{x_1}^{x_2} \quad , \tag{10}$$

where

$$y = \left(1 - 15\frac{z}{L}\right)^{1/2} \tag{11}$$

$$y' = \left(1 - 15\frac{z}{L}\right)^{1/2} \tag{12}$$

$$x = \left(1 - 15\frac{z}{L}\right)^{1/4} \quad . \tag{13}$$

Next, we compute the variations of u^*, θ^*, q^*, and L, required in the similarity equations using perturbation techniques; that is, we use linearized Taylor expansions of equations (8) through (13) and (5) and (6) as follows.

From equation (10) we can write

$$dv_2 = \frac{\partial v_2}{\partial u^*} du^* + \frac{\partial v_2}{\partial x_2} dx_2 + \frac{\partial v_2}{\partial x_1} dx_1 + \frac{\partial v_2}{\partial v_1} dv_1 \quad , \tag{14}$$

where

$$\frac{\partial v_2}{\partial u^*} = \frac{v_2 - v_1}{u^*} \tag{15a}$$

$$\frac{\partial v_2}{\partial x_2} = 4\frac{u^*}{k} \left\{ \frac{x_2^2}{x_2^4 - 1} \right\} \tag{15b}$$

$$\frac{\partial v_2}{\partial x_1} = - \frac{4u^*}{k} \left\{ \frac{x_1^2}{x_1^4 - 1} \right\} \tag{15c}$$

$$\frac{\partial v_2}{\partial v_1} = 1 \quad . \tag{15d}$$

Furthermore, since

$$x = \left(1 - 15\frac{z}{L}\right)^{1/4} \tag{16}$$

$$dx_2 = \frac{\partial x_2}{\partial z}\, dz_2 + \frac{\partial x_2}{\partial L} dL \quad , \tag{17}$$

where

$$\frac{\partial x_2}{\partial z} = \frac{15}{4L}\left(1 - 15\frac{z_2}{L}\right)^{-3/4} \quad . \tag{18a}$$

$$\frac{\partial x_2}{\partial L} = \frac{15}{4L^2}\left(1 - 15\frac{z_2}{L}\right)^{-3/4} \quad . \tag{18b}$$

Similarly for $x = x_1$

$$dx_1 = \frac{\partial x_1}{\partial z_1} dz_1 + \frac{\partial x_1}{\partial L} dL \quad , \tag{19}$$

where

$$\frac{\partial x_1}{\partial z_1} = -\frac{15}{4L}\left(1 - 15\frac{z_1}{L}\right)^{-3/4} \tag{20a}$$

$$\frac{\partial x_1}{\partial L} = -\frac{15}{4L^2}(1 - 15\frac{z_1}{L})^{-3/4} \quad . \tag{20b}$$

Substituting equations (15) through (20) into equation (14) gives

$$dv_2 - dv_1 = \frac{(v_2 - v_1)}{u^*} du^* +$$

$$\frac{15u^*}{kL^2} \left\{ \frac{z_2}{x_2(x_2^4 - 1)} - \frac{z_1}{x_1(x_1^4 - 1)} \right\} dL \tag{21}$$

$$- \frac{15u^*}{L} \left\{ \frac{dz_2}{x_2(x_2^4 - 1)} - \frac{dz_1}{x_1(x_1^4 - 1)} \right\} .$$

From equation (8), we can write

$$d\theta_2 = \frac{\partial\theta_2}{\partial\theta_1} d\theta_1 + \frac{\partial\theta_2}{\partial\theta^*} d\theta^* + \frac{\partial\theta_2}{\partial y_2} dy_2 + \frac{\partial\theta_2}{\partial y_1} dy_1 \quad , \tag{22}$$

where

$$\frac{\partial\theta_2}{\partial\theta_1} = 1 \tag{23a}$$

$$\frac{\partial\theta_2}{\partial y_2} = \frac{\theta^*}{k} \left\{ \frac{2}{(y_2^2 - 1} \right\} \tag{23b}$$

$$\frac{\partial\theta_2}{\partial y_1} = -\frac{\theta^*}{k} \left\{ \frac{2}{(y_1^2 - 1} \right\} \tag{23c}$$

$$\frac{\partial\theta_2}{\partial\theta^*} = \frac{\theta_2 - \theta_1}{\theta^*} \quad . \tag{23d}$$

Since $y = \left(1 - \frac{15}{L}\right)^{1/2}$,

$$dy = \frac{\partial y}{\partial z}dz + \frac{\partial y}{\partial L}dL \quad , \tag{24a}$$

where

$$\begin{aligned} \frac{\partial y}{\partial z} &= -\frac{15}{2L}\left(1 - 15\frac{z}{L}\right)^{-1/2} = -\frac{15}{2yL} \\ \frac{\partial y}{\partial L} &= \frac{15z}{2yL^2} \quad . \end{aligned} \tag{24b}$$

Hence,

$$dy_2 = -\frac{15}{2y_2L}dz_2 + \frac{15z_2}{2y_2L^2}dL \quad , \tag{24c}$$

and

$$dy_1 = -\frac{15}{2y_1L}dz_1 + \frac{15z_1}{2y_1L^2}dL \quad . \tag{24d}$$

From equations (22) through (24), we obtain

$$\begin{aligned} d\theta_2 = d\theta_1 &+ \frac{(\theta_2 - \theta_1)}{\theta^*}\, d\theta^* + \frac{15\theta^*}{kL^2}\left\{\frac{z_2}{y_2(y_2^2 - 1)} - \frac{z_1}{y_1(y_1^2 - 1)}\right\} \\ &- \frac{15\theta^*}{kL}\left\{\frac{dz_2}{y_2(y_2^2 - 1)} - \frac{dz_1}{y_1(y_1^2 - 1)}\right\} \quad . \end{aligned} \tag{25}$$

To evaluate equation (25), we require values of $d\theta_1$ and $d\theta_2$. These expressions are approximated by using the potential temperature expression for damp air,

$$\theta = T\left(\frac{p_o}{p}\right)^{k'}, \; k' \doteq 0.286 \quad . \tag{26}$$

The differential of θ using equation (26) is

$$d\theta = \theta \frac{dT}{T} + \theta k' \frac{dp}{P} \quad . \tag{27}$$

Therefore,

$$d\theta_1 = \theta_1 \left(\frac{dT_1}{T} + k' \frac{dp_1}{P_1} \right) \tag{28a}$$

and

$$d\theta_2 = \theta_2 \left(\frac{dT_2}{T_2} + k' \frac{dp_2}{P_2} \right) \quad . \tag{28b}$$

From equation (5), we write

$$dL = \frac{\partial L}{\partial u^*} du^* + \frac{\partial L}{\partial T_{v_1}} dT_{v_1} + \frac{\partial L}{\partial \theta_v^*} d\theta_v^* \quad , \tag{29}$$

where

$$\frac{\partial L}{\partial u^*} = \frac{2L}{u^*} \tag{30a}$$

$$\frac{\partial L}{\partial T_{v_1}} = \frac{L}{T_{v_1}} \tag{30b}$$

$$\frac{\partial L}{\partial \theta_v^*} = -\frac{L}{\theta_v^*} \quad . \tag{30c}$$

However, since

$$T_{v_1} = T_1(1 + 0.61q_1) \tag{31}$$

$$dT_{v_1} = \frac{\partial T_{v_1}}{\partial T_1} dT_1 + \frac{\partial T_{v_1}}{\partial q_1} dq_1 \quad , \tag{32}$$

where

$$\frac{\partial T_{v_1}}{\partial T_1} = (1 + 0.61q_1) \tag{33a}$$

$$\frac{\partial T_{v_1}}{\partial q_1} = 0.61T_1 \quad . \tag{33b}$$

To evaluate equations (31) and (32), we require values for q_1 and dq_1. These are obtained by using the approximations (Rogers, 1979)

$$q = \frac{3.8}{P} f \exp\left\{K\left(\frac{1}{273.16} - \frac{1}{T}\right)\right\} \tag{34}$$

$$dq = \frac{\partial q}{\partial p} dp + \frac{\partial q}{\partial f} df + \frac{\partial q}{\partial T} dT \quad , \tag{35}$$

where

$$\frac{\partial q}{\partial p} = -\frac{q}{p} \tag{36a}$$

$$\frac{\partial q}{\partial f} = \frac{q}{f} \tag{36b}$$

$$\frac{\partial q}{\partial T} = \frac{qK}{T^2} \tag{36c}$$

f = relative humidity in decimal form

K = 5.44×10^3 in c.g.s. units

Substituting equation (36) into equation (35) for $z = z_1$ gives

$$dq_1 = -\frac{q_1}{p_1}dp_1 + \frac{q_1}{f_1}df_1 + \frac{q_1 K}{T_1^2}dT_1 \quad , \tag{37}$$

where q_1 is evaluated by using equation (34).

To evaluate equation (32), we also require values of θ_v^* and $d\theta_v^*$. These are obtained using expressions presented in Rachele and Tunick (1991)

$$\theta_v^* = \theta^* + 0.61 T_1 q^* \quad , \tag{38}$$

and

$$d\theta_v^* = d\theta^* + 0.61 T_1 dq^* \quad , \tag{39}$$

where q^* and dq^* are discussed in section 2.

Substituting equations (30) through (39) into equation (29) gives

$$\begin{aligned} dL &= \frac{2L}{u^*}\, du^* \\ &+ \frac{L}{T_{v_1}}\left((1 + 0.61q_1)\; dT_1 + 0.61T_1\left(-q_1\,\frac{dp_1}{p_1} + \frac{q_1}{f_1}\, df_1 + \frac{q_1 K}{T_1^2}\, dT_1\right)\right) \\ &- \frac{L}{\theta_v^*}\,(d\theta^* + 0.61T_1 dq^*) \; . \end{aligned} \tag{40}$$

From equation (9), we write

$$dq = \frac{\partial q}{\partial q_1}dq_1 + \frac{\partial q}{\partial q^*}dq^* + \frac{\partial q}{\partial y_2'}dy_2' + \frac{\partial q}{\partial y_1}dy_1' \; , \tag{41}$$

where

$$\frac{\partial q}{\partial q_1} = 1 \tag{42a}$$

$$\frac{\partial q}{\partial q^*} = \frac{q_2 - q_1}{q^*} \tag{42b}$$

$$\frac{\partial q}{\partial y_2'} = \frac{q^*}{k}\left\{\frac{2}{(y_2'^2 - 1)}\right\} \tag{42c}$$

$$\frac{\partial q}{\partial y_1'} = -\frac{q^*}{k}\left\{\frac{2}{(y_1'^2 - 1)}\right\} . \tag{42d}$$

However, since

$$y' = \left(1 - 15\frac{z}{L}\right)^{1/2} \tag{43}$$

$$dy' = \frac{\partial y'}{\partial z}dz + \frac{\partial y'}{\partial L}dL , \tag{44}$$

where

$$\frac{\partial y'}{\partial z} = -\frac{15}{2Ly'} \tag{45a}$$

$$\frac{\partial y'}{\partial L} = \frac{15z}{2L_v^2 y'} . \tag{45b}$$

Substituting equations (42) through (45) into equation (41) gives

$$dq_2 - dq_1 = \frac{(q_2 - q_1)}{q^*} dq^* + \frac{15q^*}{kL}\left\{\frac{dz_1}{y_1'(y_1'^2 - 1)} - \frac{dz_2}{y_2'(y_2'^2 - 1)}\right\}$$

$$+ \frac{15q^*}{kL^2}\left\{\frac{z_2}{y_2'(y_2'^2 - 1)} - \frac{z_1}{y_1'(y_1'^2 - 1)}\right\} dL \ , \tag{46}$$

where

$$dq_2 - dq_1 = \left\{-q_2\frac{dp_2}{P_2} + q_2\frac{df_2}{f_2} + \frac{q_2 K}{T_2^2} dT_2 + q_1\frac{dp_1}{P_1} - q_1\frac{df_1}{f_1} - q_1\frac{KdT_1}{T_1}\right\} . \tag{47}$$

At this point, we have four equations, (21), (25), (40), and (46), in four unknowns that are driven by deviations in V, T, P, z, and f shown in matrix form. This is our solution matrix.

$$\begin{bmatrix} \gamma_{11} & 0 & 0 & \gamma_{14} \\ 0 & \gamma_{22} & 0 & \gamma_{24} \\ 0 & 0 & \gamma_{33} & \gamma_{34} \\ \gamma_{41} & \gamma_{42} & \gamma_{43} & \gamma_{44} \end{bmatrix} \begin{bmatrix} du^* \\ d\theta^* \\ dq^* \\ dL \end{bmatrix} = \begin{bmatrix} A_1 \\ A_2 \\ A_3 \\ A_4 \end{bmatrix} , \tag{48}$$

where

$$\gamma_{11} = \frac{(v_2 - v_1)}{u^*} \tag{49}$$

$$\gamma_{14} = \frac{15u^*}{kL^2}\left\{\frac{z_2}{x_2(x_2^4 - 1)} - \frac{z_1}{x_1(x_1^4 - 1)}\right\} \tag{50}$$

$$A_1 = dv_2 - dv_1 + \frac{15u^*}{kL}\left\{\frac{dz_2}{x_2(x_2^4 - 1)} - \frac{dz_1}{x_1(x_1^4 - 1)}\right\} \tag{51}$$

$$\gamma_{24} = \frac{15\theta^*}{kL^2}\left\{\frac{z_2}{y_2(y_2^2 - 1)} - \frac{z_1}{y_1(y_1^2 - 1)}\right\} \tag{52}$$

$$\gamma_{22} = \frac{(\theta_2 - \theta_1)}{\theta^*} \tag{53}$$

$$\begin{aligned} A_2 = {} & \theta_2\left(\frac{dT_2}{T_2} - k'\frac{dp_2}{P_2}\right) - \theta_1\left(\frac{dT_1}{T_1} - k'\frac{dp_1}{P_1}\right) \\ & + \frac{15\theta^*}{kL}\left\{\frac{dz_2}{y_2(y_2^2 - 1)} - \frac{dz_1}{y_1(y_1^2 - 1)}\right\} \end{aligned} \tag{54}$$

$$\gamma_{33} = \frac{(q_2 - q_1)}{q^*} \tag{55}$$

$$\gamma_{34} = \frac{15q^*}{kL^2}\left\{\frac{z_2}{y_2'(y_2'^2 - 1)} - \frac{z_1}{y_1'(y_1'^2 - 1)}\right\} \tag{56}$$

$$\begin{aligned} A_3 = {} & -q_2\left[\frac{dp_2}{P_2} - \frac{df_2}{f_2} - K\frac{dT_2}{T_2^2}\right] + q_1\left[\frac{dp_1}{P_1} - \frac{df_1}{f_1} - K\frac{dT_1}{T_1^2}\right] \\ & + \frac{15q^*}{kL}\left\{\frac{dz_2}{y_2'(y_2'^2 - 1)} - \frac{dz_1}{y_1'(y_1'^2 - 1)}\right\} \end{aligned} \tag{57}$$

$$\gamma_{41} = \frac{2L}{u^*} \tag{58}$$

$$\gamma_{42} = -\frac{L}{\theta^*} - \frac{L}{\theta_v^*} \tag{59}$$

$$\gamma_{43} = -0.61\frac{LT_{v_1}}{\theta_v^*} \tag{60}$$

$$\gamma_{44} = -1 \tag{61}$$

$$A_4 = -LdT_{v_1} \tag{62}$$

$$dT_{v_1} = (1 + 0.61q_1)\,dT_1 + 0.61T_1 dq_1 \tag{63}$$

$$dq_1 = -q_1\left(\frac{dp_1}{P_1} - \frac{df_1}{f_1} - \frac{K}{T_1^2}dT_1\right) \quad . \tag{64}$$

The matrix equation (48) is solved for randomized sets of deviations of T, P, V, f, and sensor positions, resulting in distributions of du^*, dL, $d\theta^*$, and dq^*.

Simultaneously, we compute C_n^2 for each sample set resulting in a distribution of C_n^2. The formulation we use for evaluating C_n^2 (see Rachele and Tunick, 1991) is

$$C_n^2 = A'\theta^{*2} + B'\theta^* q^* + C'q^{*2} \quad , \tag{65}$$

where

$$A' = b(6.241 \times 10^{-9})\,\frac{P^2}{T^4}K^{-2/3}z^{-2/3}\left(1 - \gamma\frac{Z}{L}\right)^{-1}\{\ \ \} \tag{66}$$

$$B' = b[3.11 \times 10^{-9}]\,\frac{P^2}{T^3} k^{-2/3} z^{-2/3}\left(1 - \gamma\frac{z}{L}\right)^{-1}\{\,\} \tag{67}$$

$$C' = b(3.88 \times 10^{-10})\,\frac{P^2}{T^2} k^{-2/3} z^{-2/3}\left(1 - \gamma\frac{z}{L}\right)^{-1}\{\,\} \tag{68}$$

$$\{\,\} = \left\{\frac{\left(1 - \gamma\,\frac{z}{L}\right)^{1/2}}{\left[\left(1 - \beta\,\frac{z}{L}\right)^{-1/4} - \frac{z}{L}\right]^{1/3}}\right\} \tag{69}$$

where

b = 3.2

$\beta = \gamma = 15$

3. RECEIVER COHERENCE DIAMETER (r_o)

The formulation we use for computing the receiver coherence diameter is discussed in Miller and Ricklin (1990),

$$r_o(\Gamma) = \left(0.423k^2 \int_\gamma C_n^2(s)\,Q_1(s)\,ds\right)^{-3/5} , \tag{70}$$

where

ds = a path length increment

Γ = propagation path

K = wave number

$Q_1(s) = \left(\frac{s}{L}\right)^{5/3}$ for a spherical wave

L = the total path length

4. THE MODULATION TRANSFER FUNCTION

The modulation transfer function (MTF) selected for this study is also discussed in Miller and Ricklin (1990). In particular, Miller and Ricklin refer to it as the near- and far-field slow turbulence modulation transfer functions (TMTF),

$$TMTF_1(f,r) = \exp\left\{-3.44\left[\frac{\lambda R f}{r_o}\right]^{5/3}\right\} \quad , \tag{71}$$

where R is the focal length, λ is the wavelength, and f is the spatial frequency.

5. EXAMPLES

For this study, we selected two sets of data from Davis, California, during unstable conditions with clear skies (Stenmark and Drury, 1970). The first case was chosen to emphasize the effects on atmospheric stability of moderate (5.0 to 7.0 m/s) winds. The second case contains lighter (2.0 to 3.0 m/s) winds and somewhat intensified atmospheric instability. The Davis field site (a flat, 5-ha area at 17 m above sea level) is located about 2 km west of the main portion of the University of California at the Davis Campus, 24 km west of Sacramento and 113 km northeast of San Francisco. The data were taken during periods when the surrounding fields, for the most part, were crop covered and well irrigated, giving, in effect, homogeneous surface conditions with respect to temperature and moisture. Advection effects were considered to be negligible. Profiles of wind, temperature, and specific humidity were measured at nine levels from 25 to 600 cm. Raw data were processed to give one-half hour average profiles. Table 1 gives the two-level (1 and 10 m) values for windspeed, temperature, specific humidity, relative humidity, and pressure for the two data sets discussed above. From these data we found values of the friction velocity u*, the potential temperature and specific humidity scaling parameters θ* and q*, and the Obukhov lengths L and L_v, which are also given in table 1.

TABLE 1. MICROMETEOROLOGICAL PARAMETERS FROM THE DAVIS, CA, DATA

	Case 1	Case 2
Date	2 Jun 66	3 Jun 66
Time (PST)	1430	1200
Windspeed (1 m)	4.48 (m/s)	2.08 (m/s)
Windspeed (10 m)	7.39 (m/s)	2.98 (m/s)
Temperature (1 m)	21.20 (°C)	21.41 (°C)
Temperature (10 m)	20.656 (°C)	20.92 (°C)
Specific humidity (1 m)	5.99×10^{-3} (g/g)	5.76×10^{-3} (g/g)
Specific humidity (10 m)	4.42×10^{-3} (g/g)	4.39×10^{-3} (g/g)
Relative humidity (1 m)	37.6 %	35.6 %
Relative humidity (10 m)	27.3 %	28.01 %
Pressure (1 m)	1000 (mbar)	1000 (mbar)
Pressure (10 m)	998.96 (mbar)	998.958 (mbar)
u* (cm/s)	53.72	20.98
θ* (K)	-0.1049	-0.1527
q* (g/g)	-3.237×10^{-4}	-4.954×10^{-4}
L (m)	-206.53	-21.64

6. RESULTS

As in our earlier report, we caution the reader to a possible pitfall of misinterpretation and application of the data presented in this report. The so-called natural variations used in this study were not determined from field data; instead they are creations on our part of what we felt were reasonable. In particular we not only required that the distributions of the fluctuations be normally distributed, but we also specified the values of the variances. (Note however that the mean values were determined from field data--see section 5.) The standard deviation for the windspeed distributions was specified to be 3.33 cm/s. We did not try to adjust the windspeed variance to changes in the magnitude of the windspeed itself. The standard deviation of temperature was chosen to be 0.033 K. The standard deviation of relative humidity was one-half of 1 percent relative humidity, and the standard deviation for the pressure was 0.33 mbar.

For each case we computed distributions of u^*, θ^*, q^*, and L. We then computed distributions of C_n^2 and r_0 (receiver coherence diameter). Finally, we derived the near- and far-field slow MTF from the minimum, maximum, and mean r_0 and plotted the slant path case (1 km length by 20 m height) for a beam pointed upward to a target and for a beam pointed downward.

The results of the two cases presented in this section are at best representations of the sensitivity of C_n^2 and subsequently r_0 and MTF to the input parameters, as specified, and should not be interpreted as real world solutions.

Figure 1* shows the two-level model (Case 1) normal distributions for H, L′E, U*, and V_r and is presented to show the fidelity of the normal distributions generated and used as input parameters.

Figure 2 shows the derived distributions for T^* (θ^*), q^*, and L. The range for these distributions is approximately a factor of 2. Note that for this case one, since U^* is relatively large and T^* is small, the mean value for the Obukhov scaling length is quite large, indicative of weakly unstable atmospheric conditions.

Figure 3 illustrates the random distribution for C_n^2 resulting from variations in u^*, θ^*, q^*, L, and V_r. The range for the random distributions of C_n^2 is approximately a factor of 3. Additionally, a cumulative distribution for C_n^2 is shown. It suggests that about 47 percent of the time C_n^2 will have a value equal to or less than its mean value.

Figures 4 and 5 show the distribution of r_0 and its effect on the MTF for Case 1. Note that the variations of the MTF are based on extreme values of r_0. Figure 4 gives the MTF for a slant path looking upward, and figure 5 shows the MTF for a slant path looking downward.

*Figures are presented at the end of the text.

Figures 6 and 7 show the distributions of V_r, U^*, T^*, q^*, and L for Case 2, and figure 8 shows C_n^2 for Case 2. Note here that mean values for T^* and q^* are slightly greater in magnitude than those from Case 1, and the mean value for U^* is small. This results in L values smaller in magnitude for this case, representing more moderately unstable atmospheric conditions. C_n^2 is significantly larger in magnitude (that is, on the order of 10^{-13}) and its range is approximately a factor of 5.

7. SUMMARY AND CONCLUSIONS

The purpose of this study was to examine the sensitivity of the receiver coherence diameter, r_o, and the MTF for deviations of C_n^2 due to variations of the natural atmosphere and from misrepresentations of the atmosphere due to errors in measurement and processing of the basic parameters involved. We selected two sets of data from Davis, California, taken during unstable conditions under clear skies. We presented graphs illustrating the derived distributions of the similarity scaling parameters, C_n^2, r_o, and plots of the MTF for two slant path situations.

We found that for the specified variations of V_r, T, P, and f that C_n^2 could be determined within a factor of 3 for Case 1 and a factor of 5 for Case 2.

The question remains as to what are acceptable ranges or values for C_n^2. The answer lies wholly with their use, or, that is, it depends on the application for C_n^2. We found for instance that r_o, the *receiver coherence diameter*, can vary from 1.26 to 3.76 cm for Case 1, causing, in turn, a significant effect upon the near- and far-field slow MTF. For Case 2 r_o varied from 3 to 6 and also resulted in more skewed distributions of MTF.

In conclusion we feel confident that our methodology was a sound indicator of potential variations in optical parameters in our models. Needless to say, a more thorough study should be performed using more complete field data.

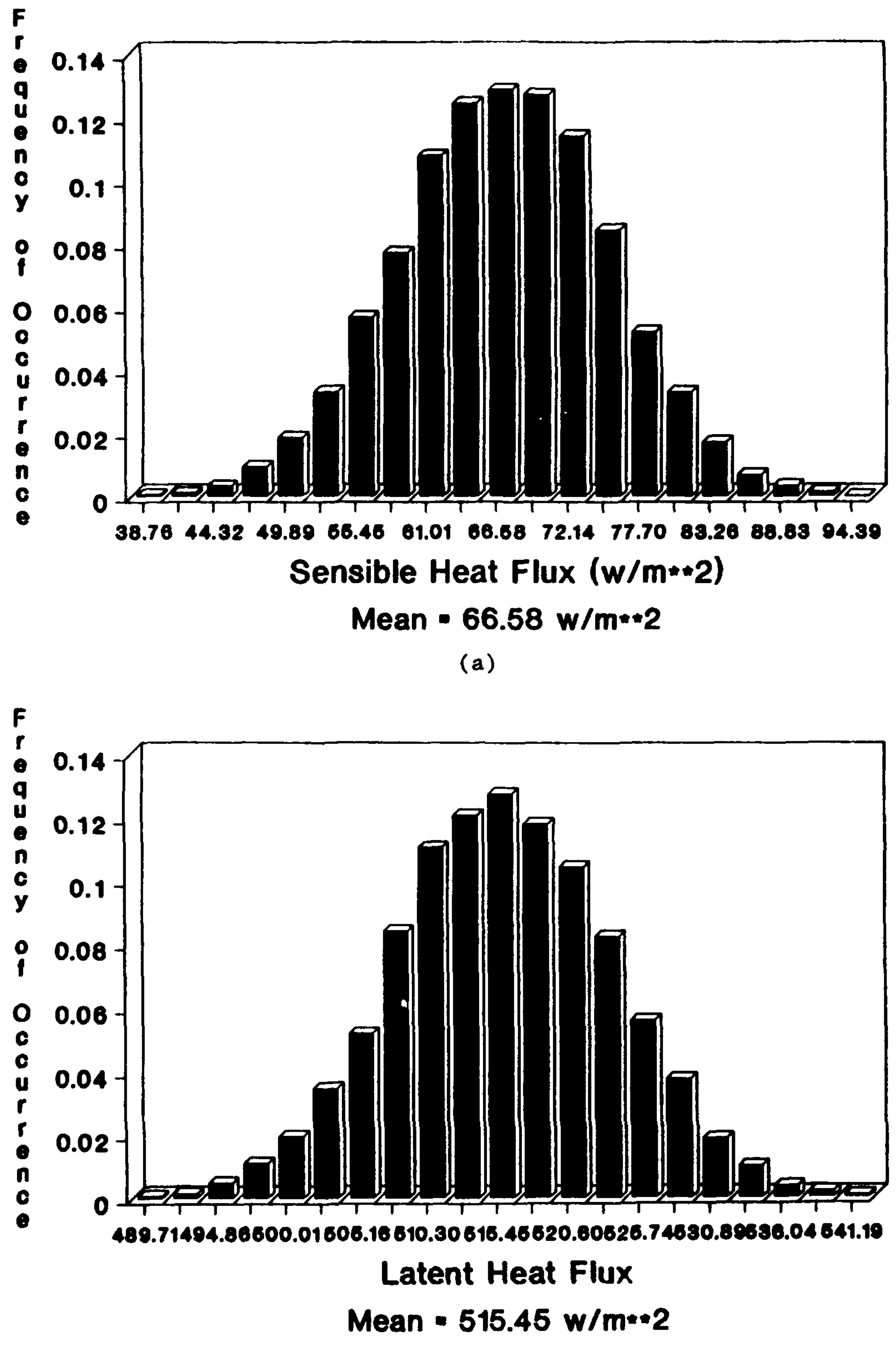

Figure 1. Case 1 - Random distribution for: (a) u* and (b) normal distribution for V_r.

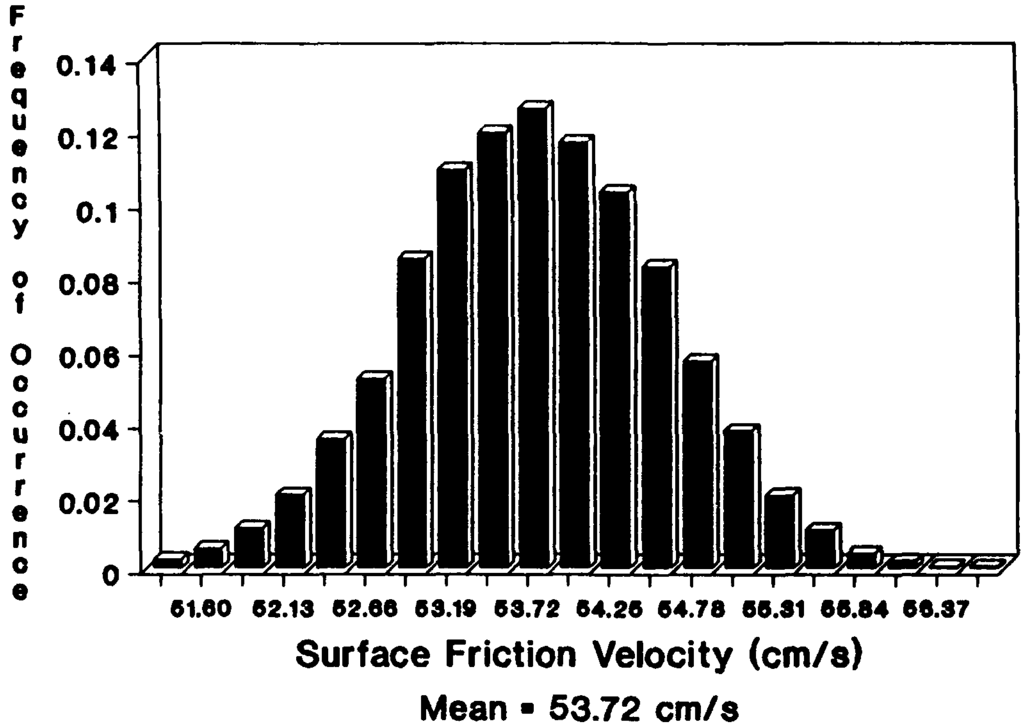

(c)

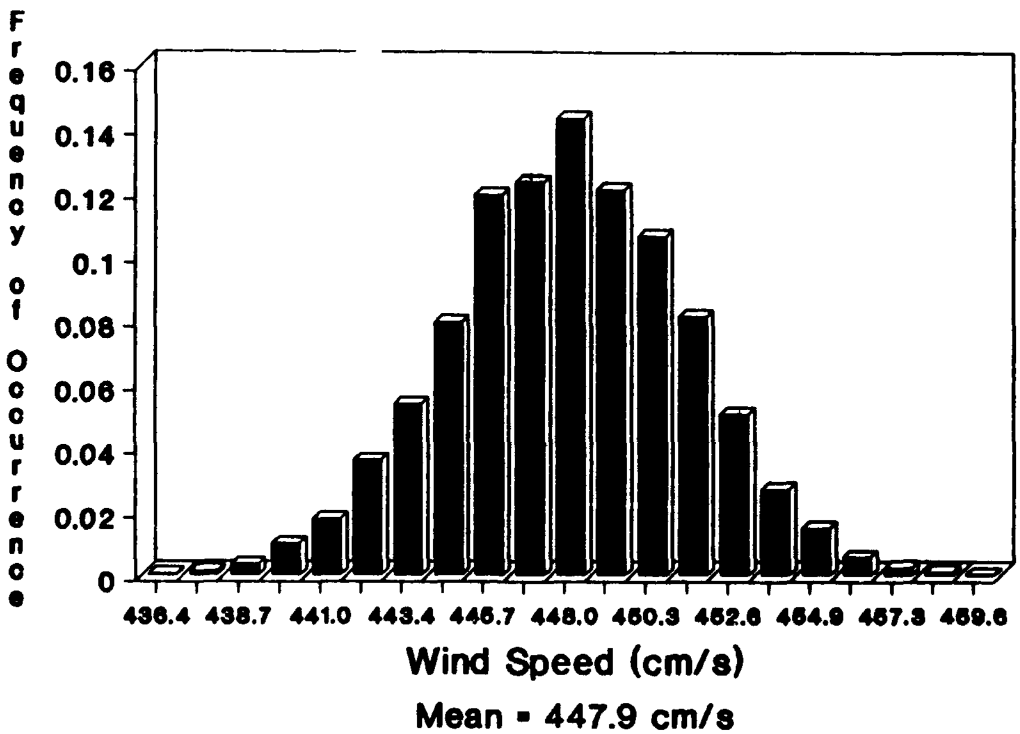

(d)

Figure 1. (cont.)

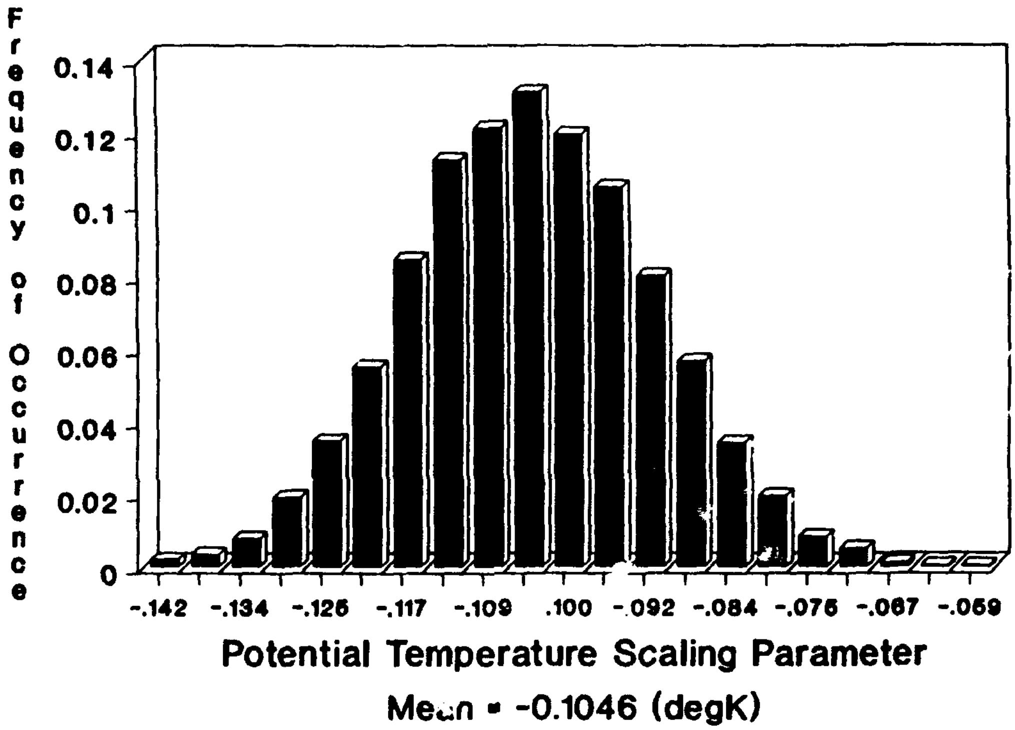

(a)

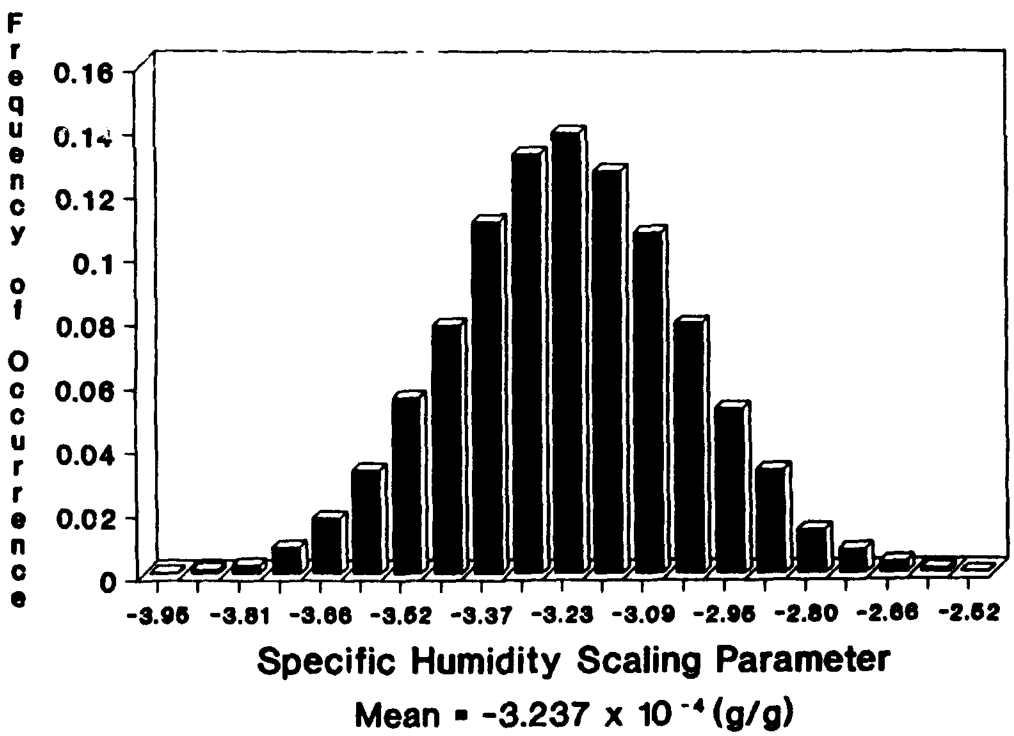

(b)

Figure 2. Case 1 - Random distribution for:
(a) T*, (b) q*, and (c) L.

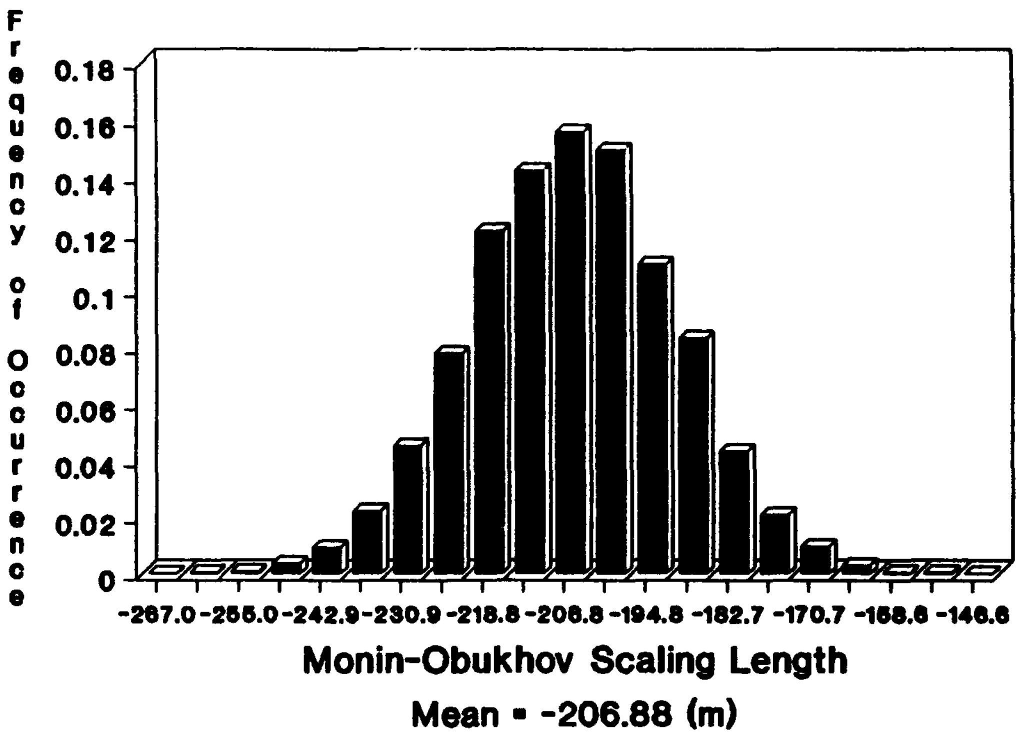

(c)

Figure 2. (cont)

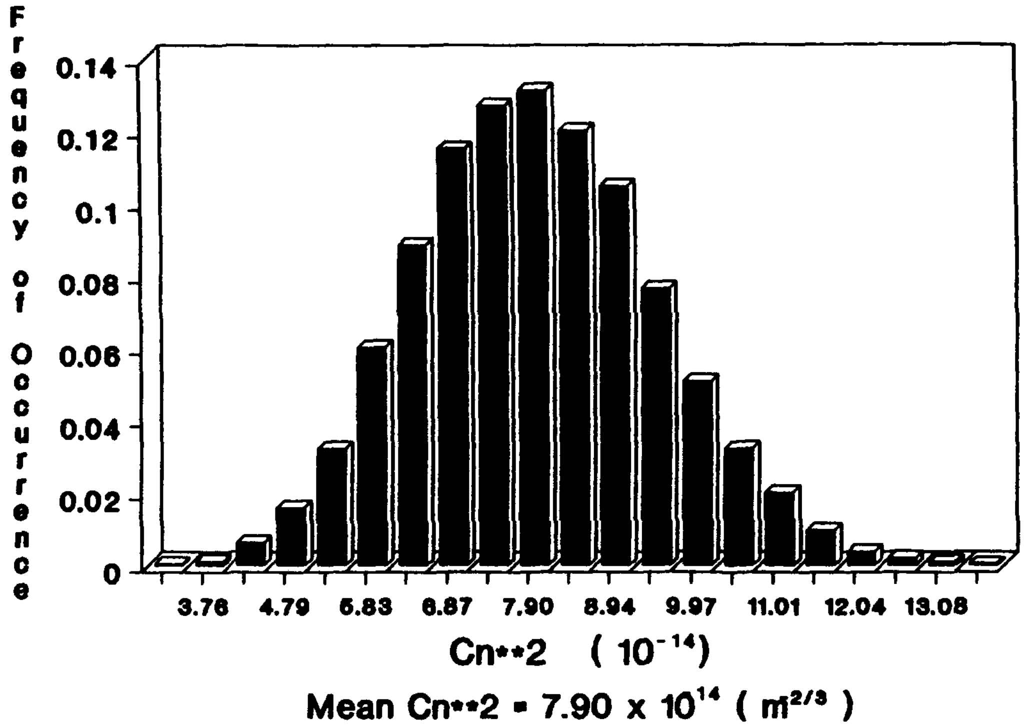

(a)

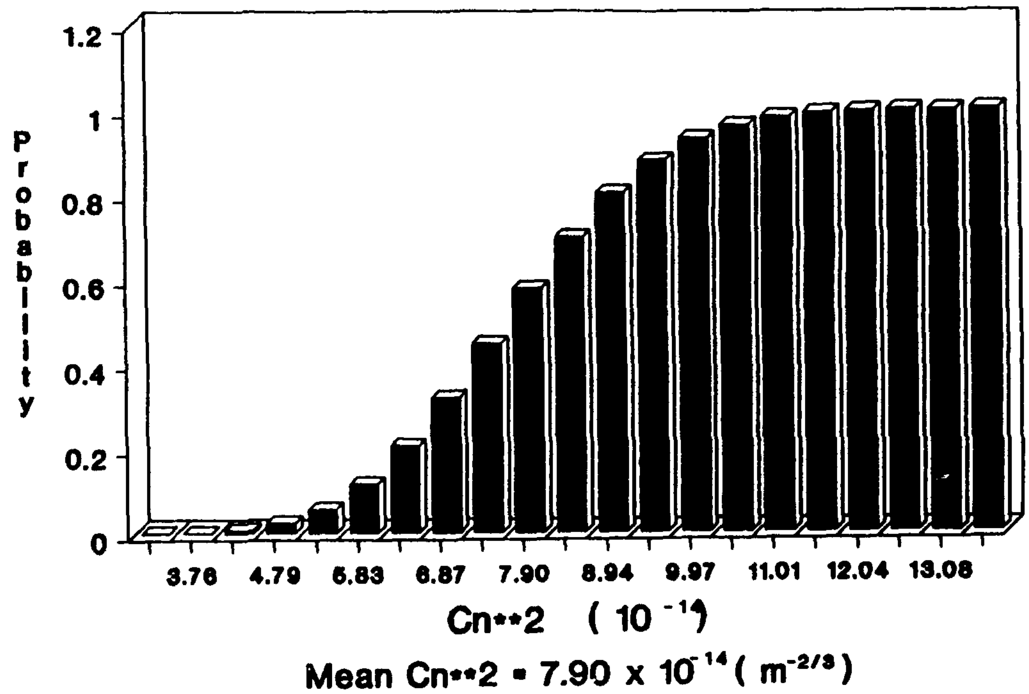

(b)

Figure 3. Case 1 - Distribution for C_n^2:
(a) random and (b) probability.

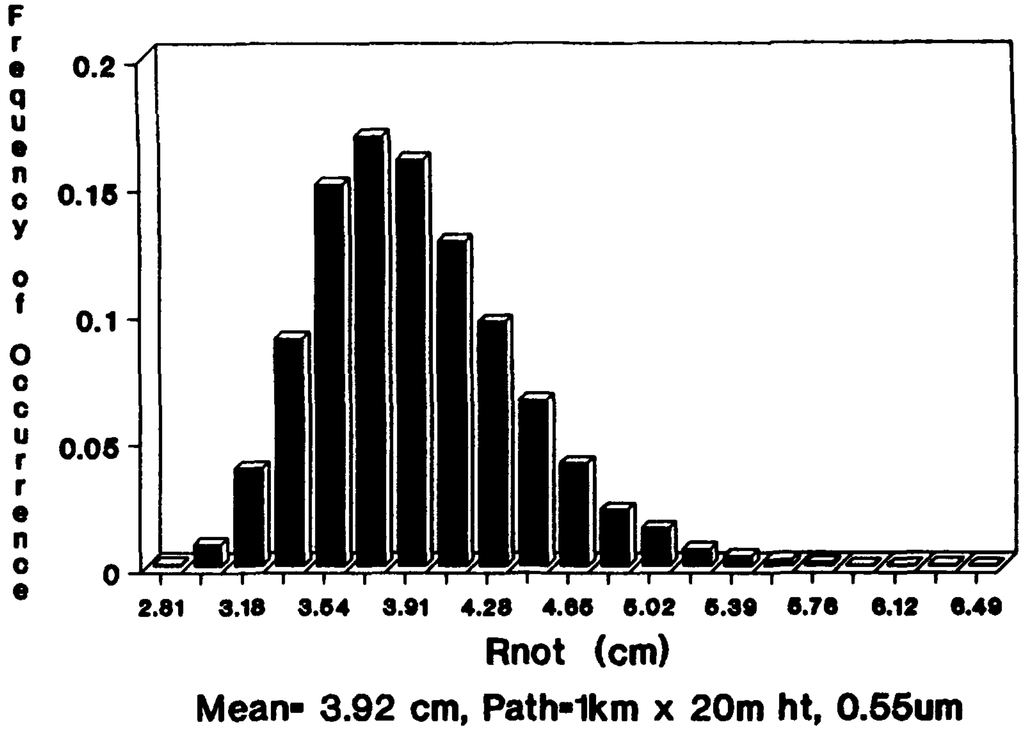

(a)

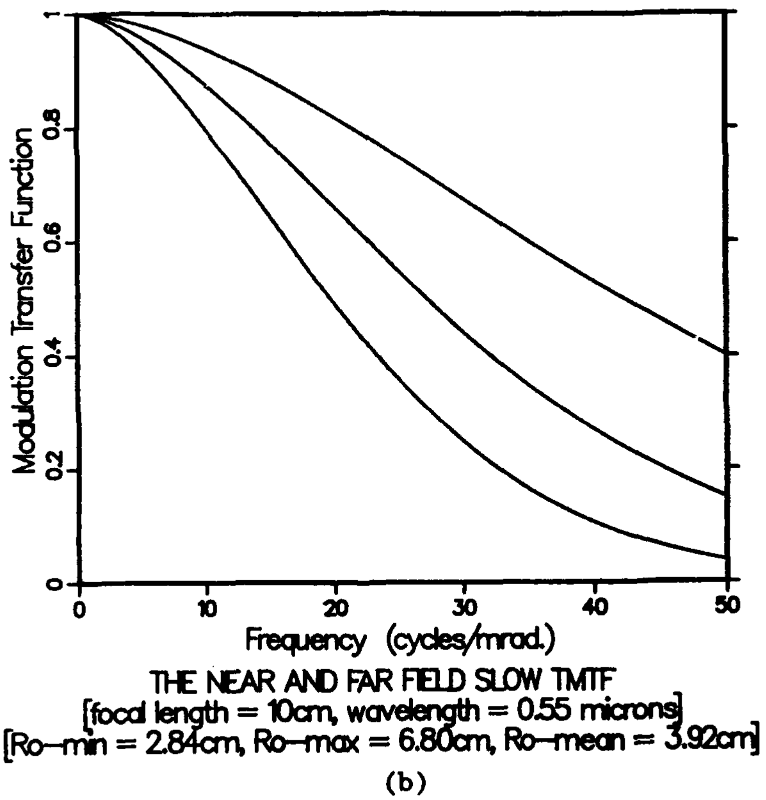

(b)

Figure 4. Case 1 - (a) Random distribution for r_o and (b) the resultant MTF for a slant path looking upward.

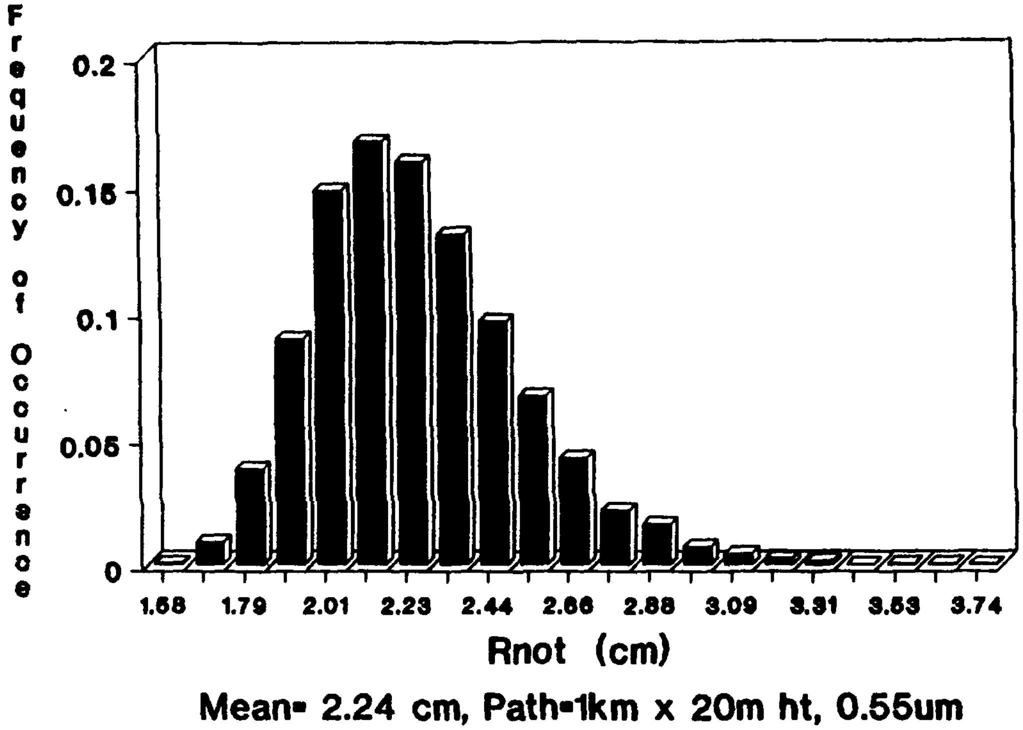

(a)

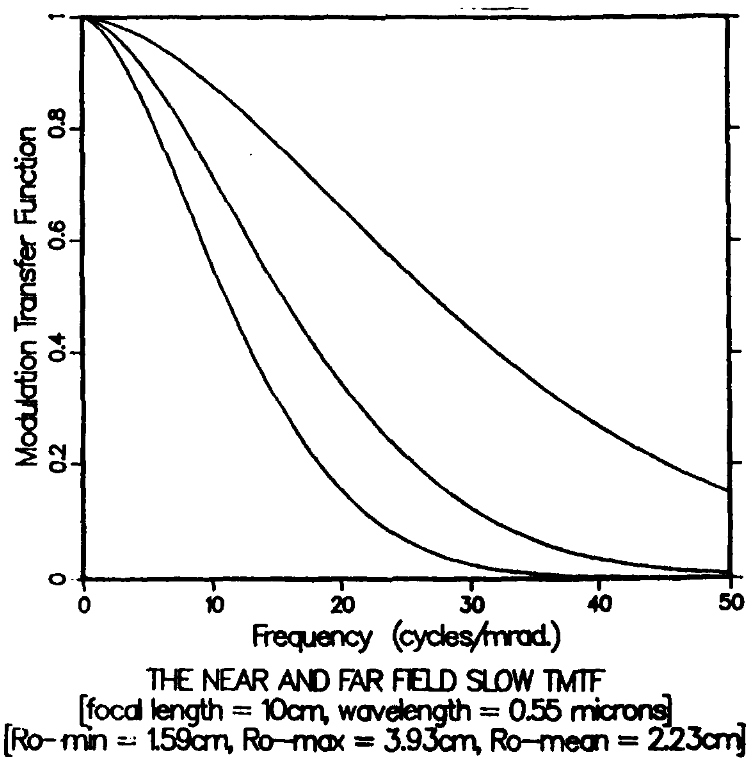

(b)

Figure 5. Case 1 - (a) Random distribution for r_o and (b) the resultant MTF for a slant path looking downward.

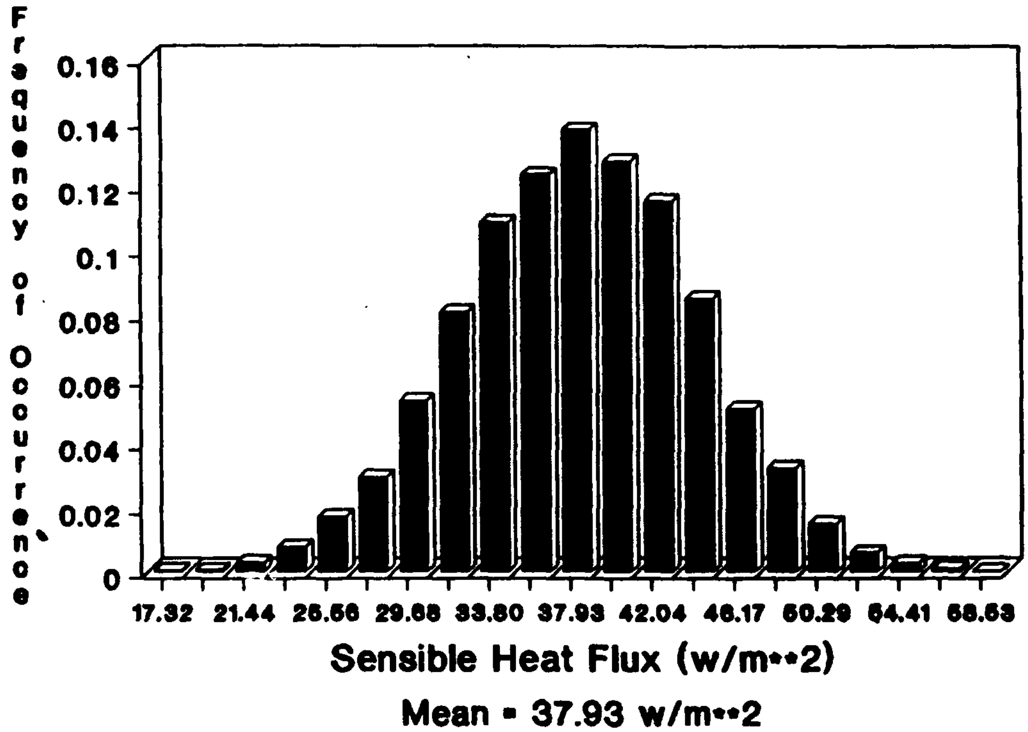

(a)

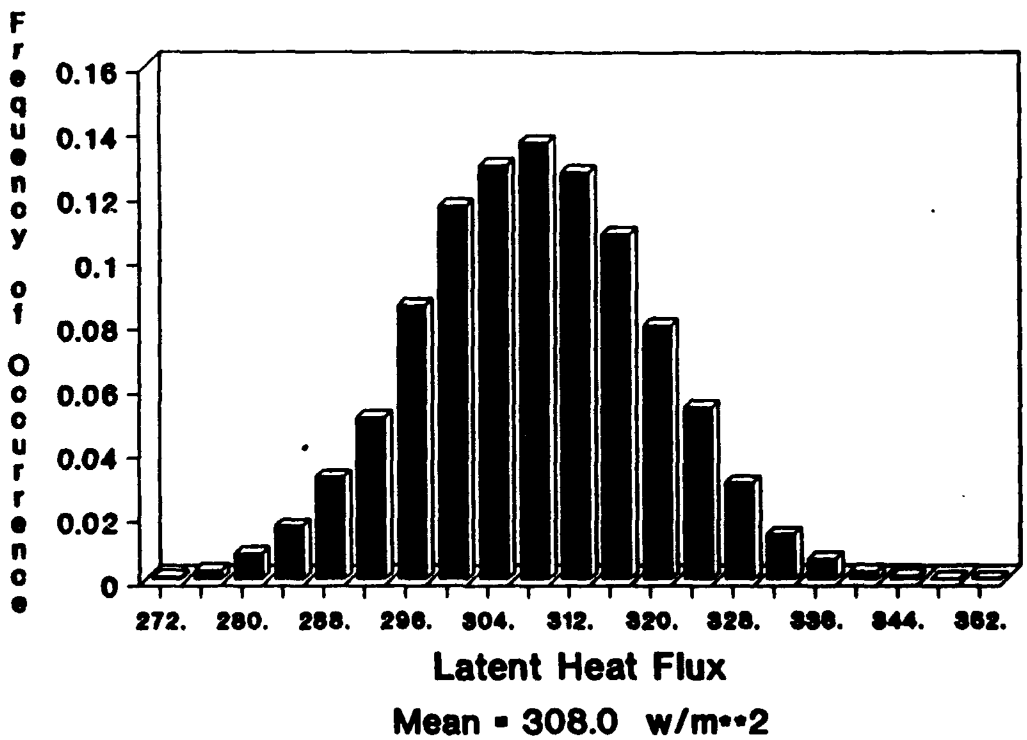

(b)

Figure 6. Case 2 - Random distribution for: (a) u* and (b) normal distribution for V_r.

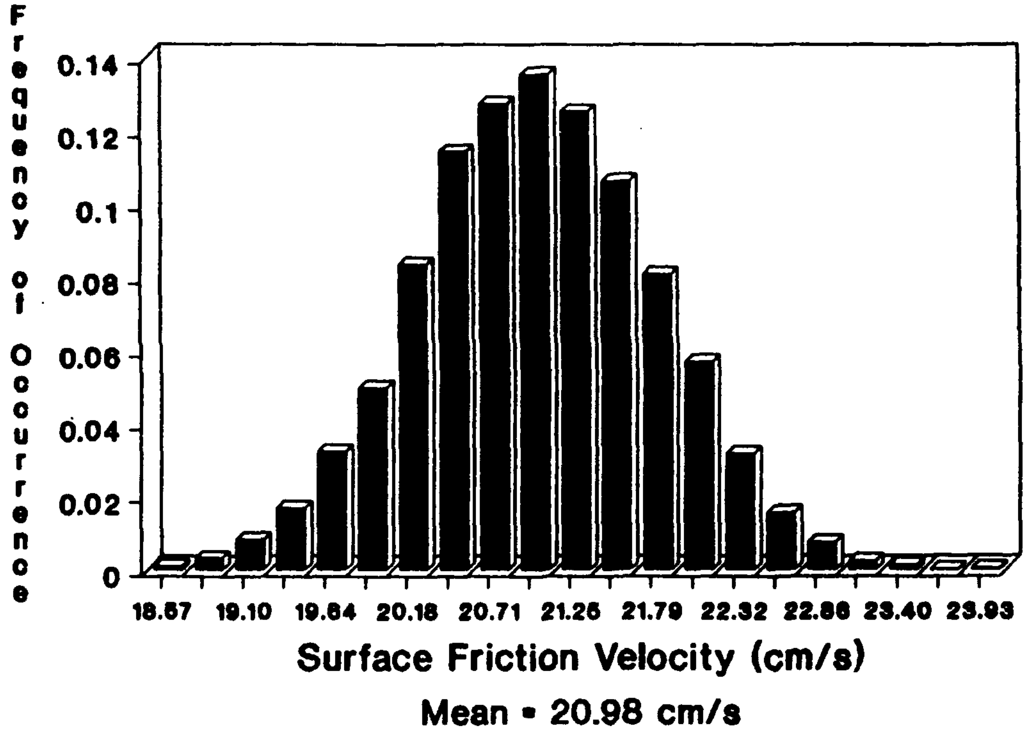

(c)

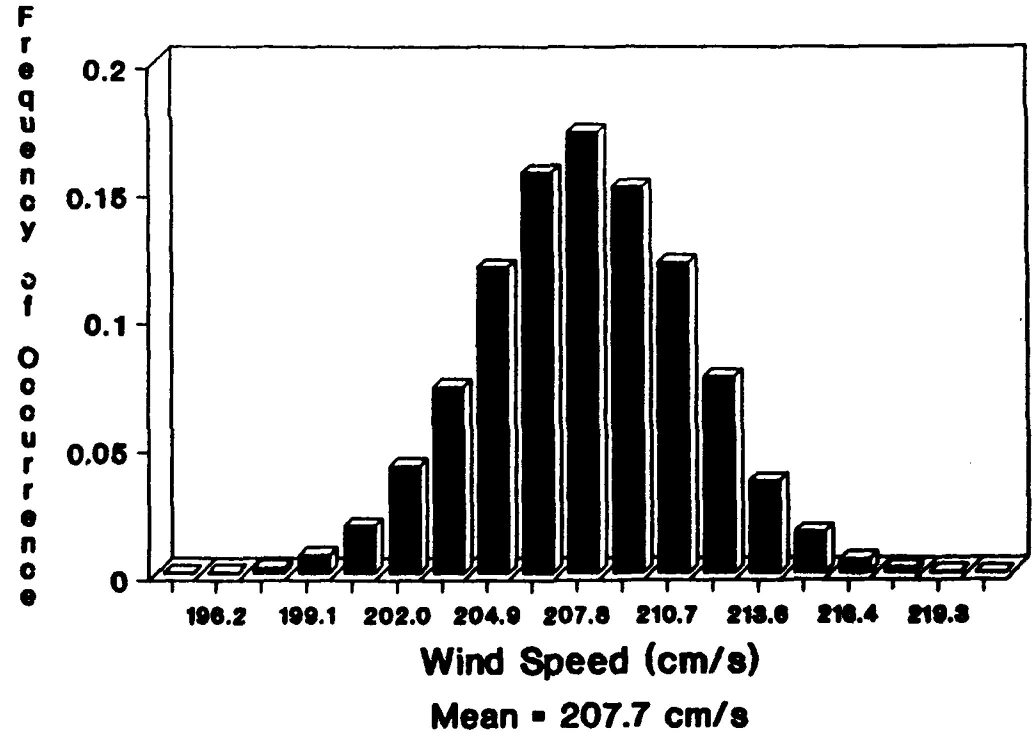

(d)

Figure 6. (cont)

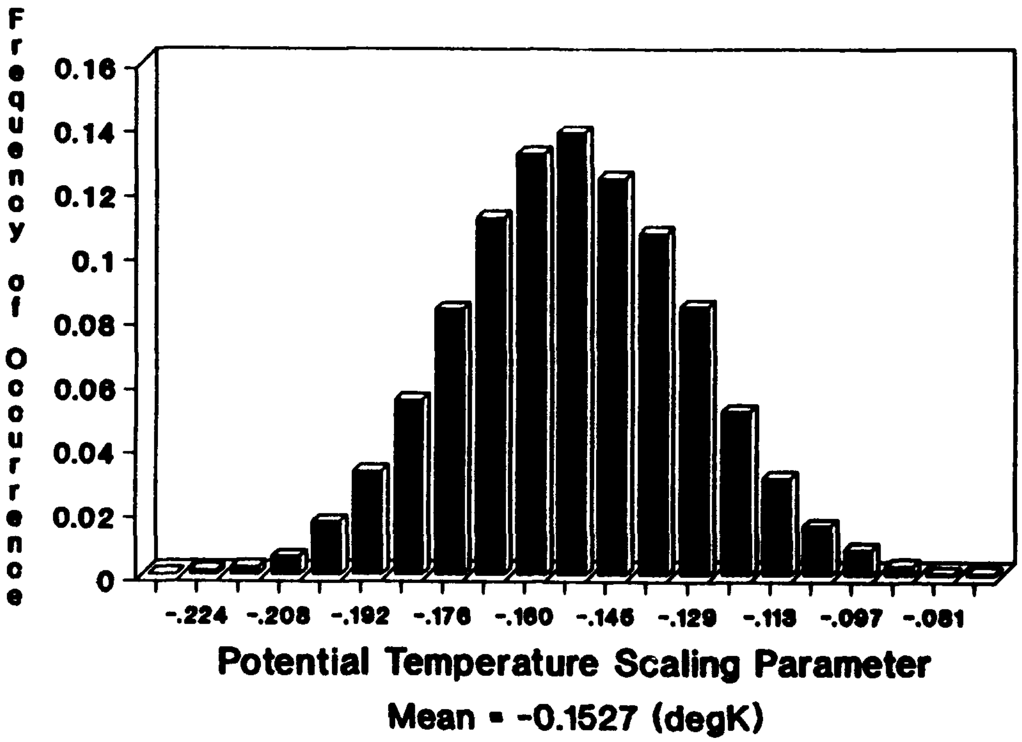

(a)

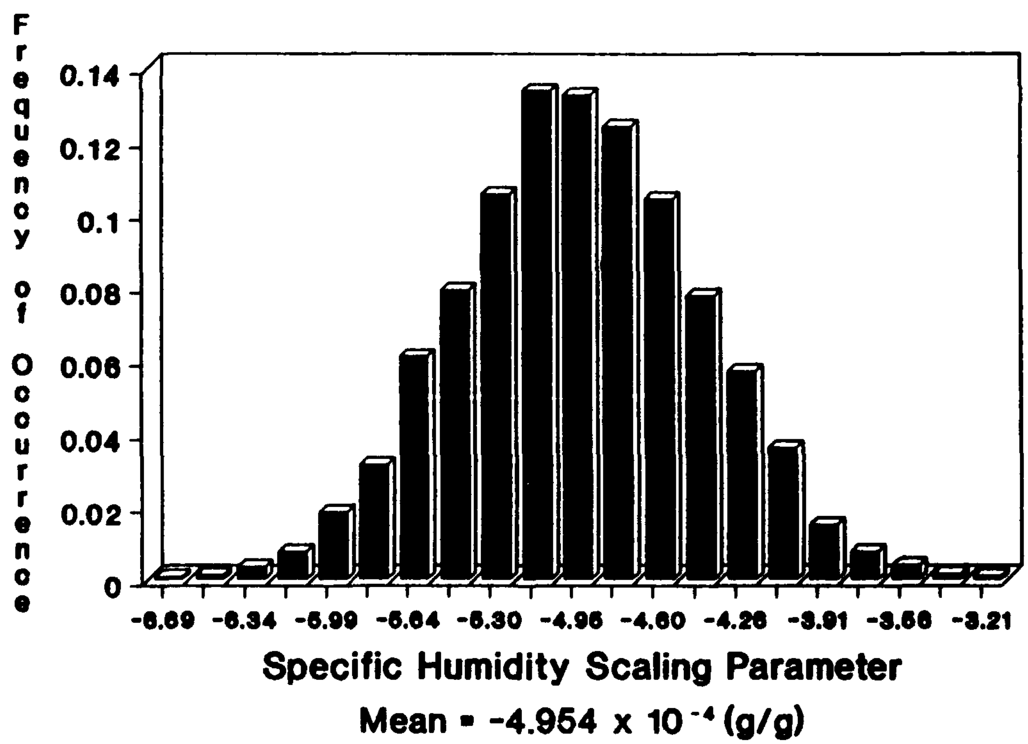

(b)

Figure 7. Case 2 - Random distribution for: (a) T*, (b) q*, and (c) L.

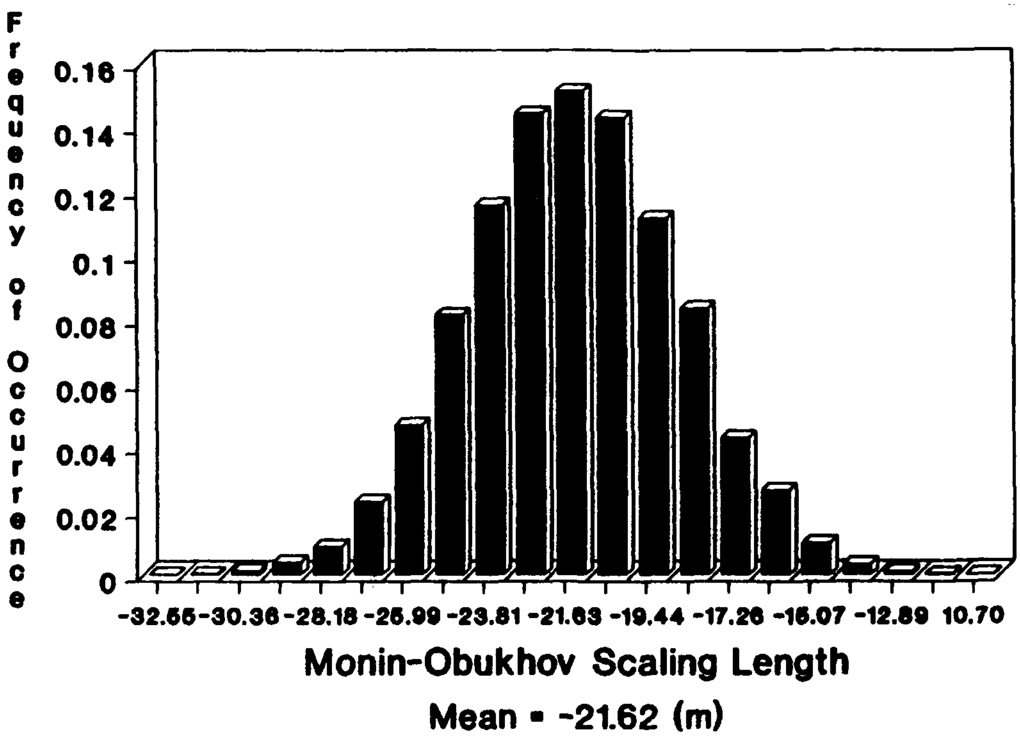

(c)

Figure 7. (cont)

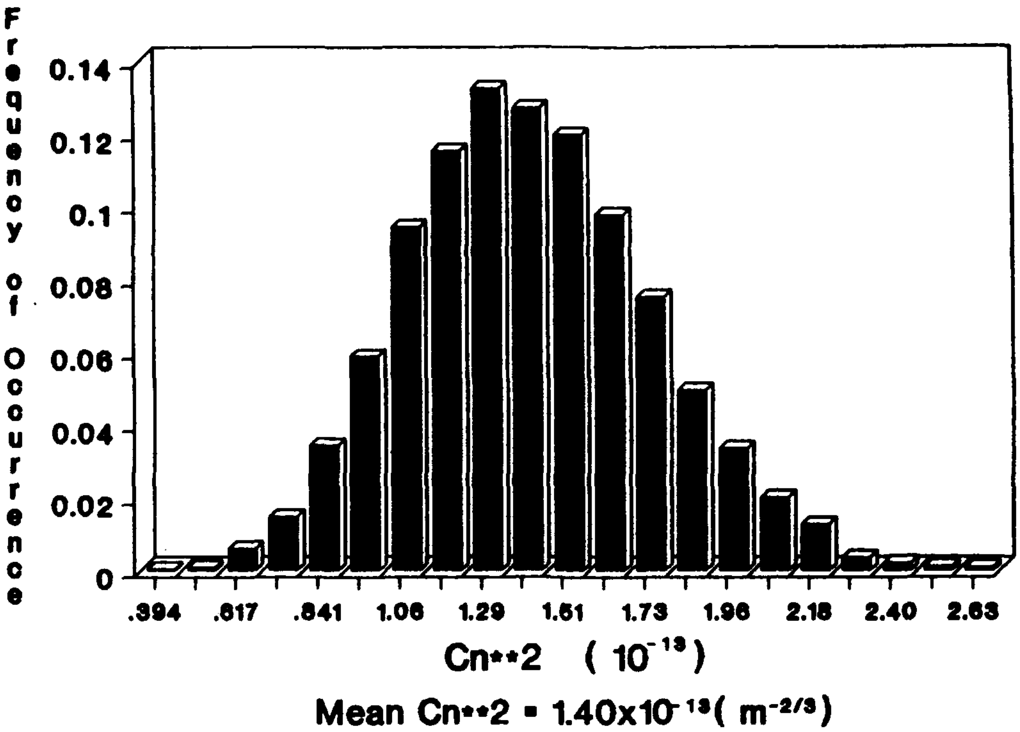

(a)

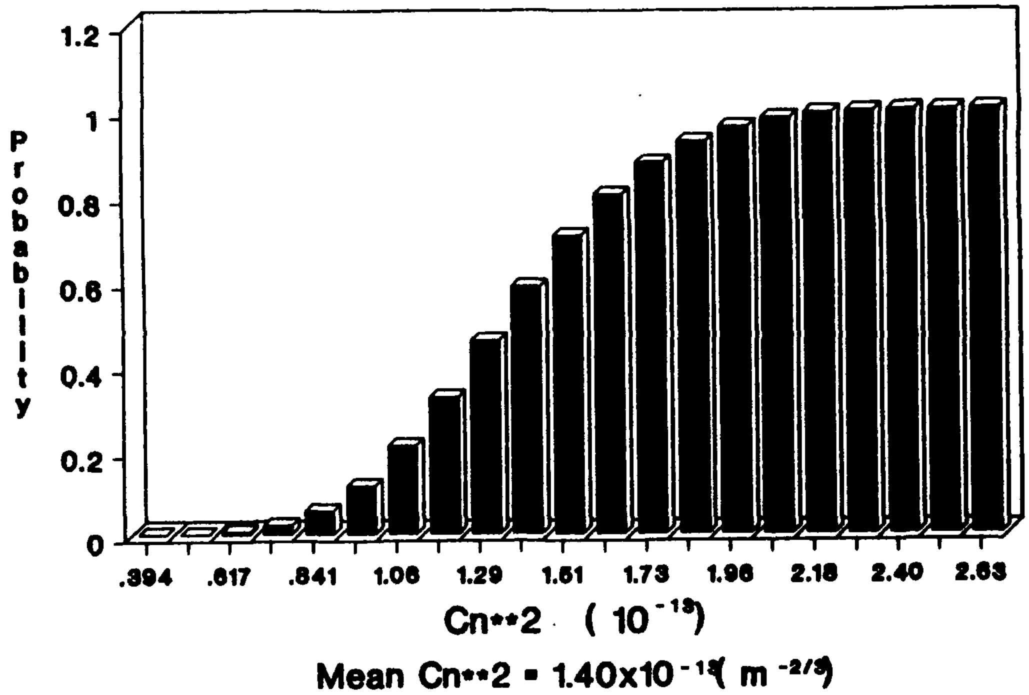

(b)

Figure 8. Case 2 - Distribution for C_n^2:
(a) random and (b) probability.

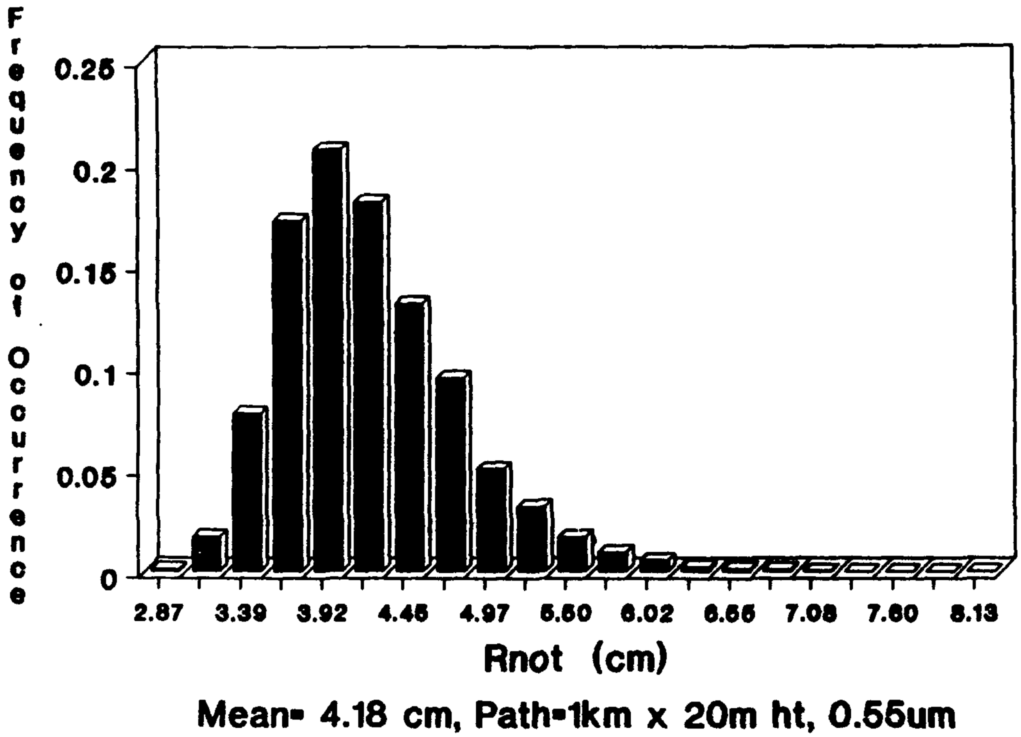

(a)

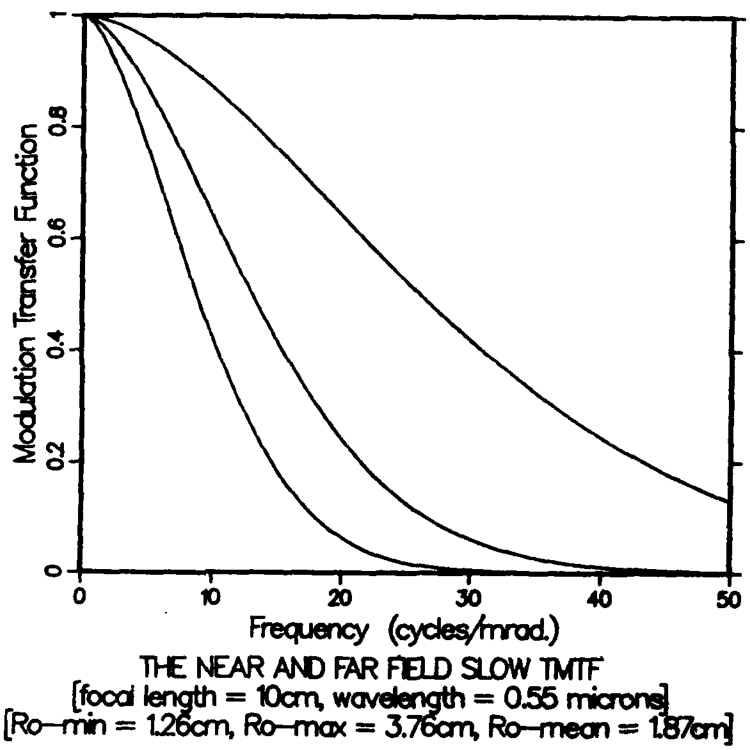

(b)

Figure 9. Case 1 - (a) Random distribution for r_0 and (b) the resultant MTF for a slant path looking upward.

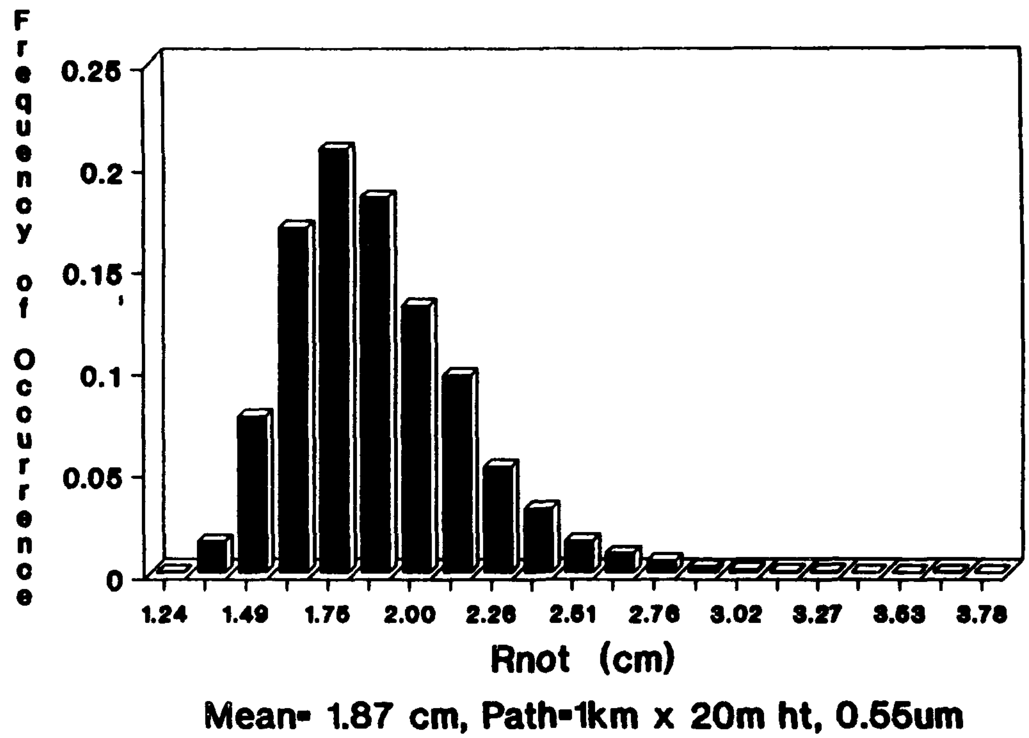

(a)

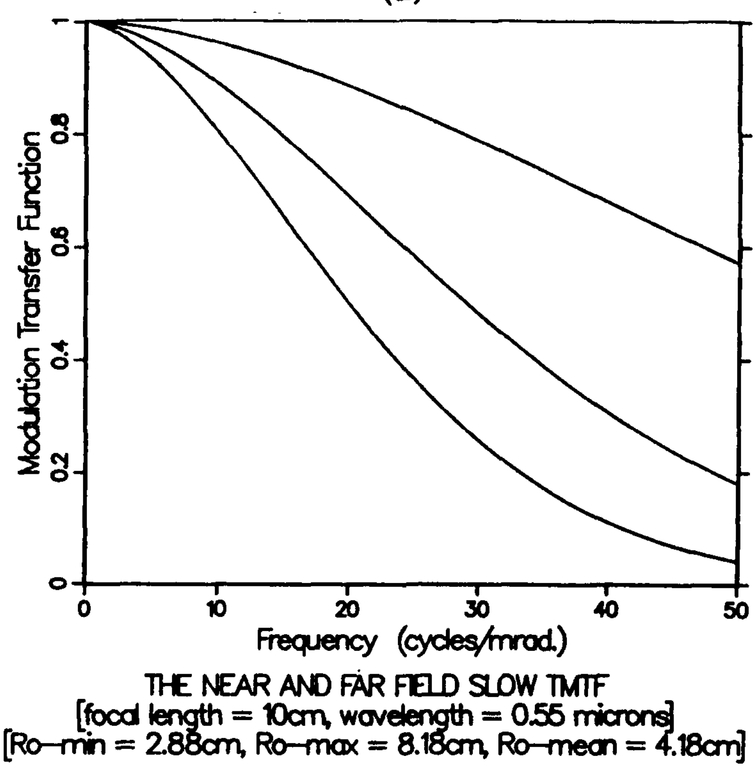

(b)

Figure 10. Case 1 - (a) Random distribution for r_0 and (b) the resultant MTF for a slant path looking downward.

LITERATURE CITED

Andreas, Edgar L., 1988, "Estimating C_n^2 over Snow and Sea Ice from Meteorological Data," J Opt Soc Am, 5:481-495.

Hill, R. J., 1989, "Implementation of Monin-Obukhov Similarity Theory for Scalor Quantities, "J Atmos Sci, 46:2236.2244.

Izumi, Y., 1971, Kansas 1968 Field Program Data Report, AFCRL-72-0041, Air Force Cambridge Research Laboratories, L. G. Hanscom Field, Bedford, MA.

Lumley, J. L., and H. A. Panofsky, 1964, The Structure of Atmospheric Turbulence, J. Wiley and Sons, New York, London, Sydney.

Miller, W. B., and J. C. Ricklin, 1990, EOSAEL 87, A Module for Imaging Through Optical Turbulence, IMTURB, ASL-TR-0221-27, U.S. Army Atmospheric Sciences Laboratory, White Sands Missile Range, NM.

Obukhov, A. M., 1946, "Turbulence in an Atmosphere of Nonhomogeneous Temperature," Trans Inst Theort Geophys, USSR, 1:95.

Panofsky, H. A., 1968, "The Structure Constant for the Index of Refraction in Relation to the Gradient of Index of Refraction in the Surface Layer," J Geophys Res, 73(18):6047-6049.

Pries, T., and J. F. Appleby, 1967, The Distribution of Eddy Velocities and Temperature Fluctuations in the First 100 Meters, ECOM-6027, U.S. Army Atmospheric Sciences Laboratory, Fort Huachuca, AZ.

Rachele, H., and A. Tunick, 1992, Sensitivity of C_n^2 Random Variations of Windspeed, Sensible Heat Flux, and Latent Heat Flux, ASL-TR-0308, U.S. Army Atmospheric Sciences Laboratory, White Sands Missile Range, NM.

Rachele, H., and A. Tunick, 1991, Estimating C_n^2, C_T^2, C_{Tq}, and C_q^2 During Unstable Atmospheric Conditions, ASL-TR-0299, U.S. Army Atmospheric Sciences Laboratory, White Sands Missile Range, NM.

Rogers, R. R., 1979, A Short Course in Cloud Physics, Second Edition, Pergamon Press, New York-Toronto-Sydney.

Stenmark, E. B., and L. D. Drury, 1970, Micrometeorological Field Data from Davis, California: 1966-67, Runs under Non-Advective Conditions, ECOM-6051, U.S. Army Atmospheric Sciences Laboratory, Fort Huachuca, AZ.

Tatarski, V. I., 1961, Wave Propagation in a Turbulent Medium, McGraw-Hill Book Co., Inc., New York-Toronto-London.

Tunick, A., H. Rachele, and W. B. Miller, 1990, "C_n^2 Estimates in the Boundary Layer for Damp Unstable Conditions," in Proceedings of the Eleventh Annual EOSAEL/TWI Conference, U.S. Army Atmospheric Sciences Laboratory, White Sands Missile Range, NM.

Tunick, A., and H. Rachele, 1991, "Estimating the Effects of Temperature and Moisture on C_n^2 in the Damp Unstable Boundary Layer for Visible Infrared, Radio, and MM Wavelengths," in Proceedings of the 1991 Battlefield Atmospherics Conference, U.S. Army Atmospheric Sciences Laboratory, White Sands Missile Range, NM.

Wyngaard, J. C., 1973, "On Surface-Layer Turbulence," Workshop on Micrometeorology, D. A. Haugen, ed., American Meteorological Society, Boston, MA, pp 101-149.

DISTRIBUTION LIST FOR PUBLIC RELEASE

Commandant
U.S. Army Chemical School
ATTN: ATZN-CM-CC (S. Barnes)
Fort McClellan, AL 36205-5020

Commander
U.S. Army Aviation Center
ATTN: ATZQ-D-MA
Mr. Oliver N. Heath
Fort Rucker, AL 36362

Commander
U.S. Army Aviation Center
ATTN: ATZQ-D-MS (Mr. Donald Wagner)
Fort Rucker, AL 36362

NASA/Marshall Space Flight Center
Deputy Director
Space Science Laboratory
Atmospheric Sciences Division
ATTN: E501 (Dr. George H. Fichtl)
Huntsville, AL 35802

NASA/Marshall Space Flight Center
Atmospheric Sciences Division
ATTN: Code ED-41
Huntsville, AL 35812

Deputy Commander
U.S. Army Strategic Defense Command
ATTN: CSSD-SL-L
Dr. Julius Q. Lilly
P.O. Box 1500
Huntsville, AL 35807-3801

Commander
U.S. Army Missile Command
ATTN: AMSMI-RD-AC-AD
Donald R. Peterson
Redstone Arsenal, AL 35898-5242

Commander
U.S. Army Missile Command
ATTN: AMSMI-RD-AS-SS
Huey F. Anderson
Redstone Arsenal, AL 35898-5253

Commander
U.S. Army Missile Command
ATTN: AMSMI-RD-AS-SS
B. Williams
Redstone Arsenal, AL 35898-5253

Commander
U.S. Army Missile Command
ATTN: AMSMI-RD-DE-SE
Gordon Lill, Jr.
Redstone Arsenal, AL 35898-5245

Commander
U.S. Army Missile Command
Redstone Scientific Information
Center
ATTN: AMSMI-RD-CS-R/Documents
Redstone, Arsenal, AL 35898-5241

Commander
U.S. Army Intelligence Center
and Fort Huachuca
ATTN: ATSI-CDC-C (Mr. Colanto)
Fort Huachuca, AZ 85613-7000

Northrup Corporation
Electronics Systems Division
ATTN: Dr. Richard D. Tooley
2301 West 120th Street, Box 5032
Hawthorne, CA 90251-5032

Commander - Code 3331
Naval Weapons Center
ATTN: Dr. Alexis Shlanta
China Lake, CA 93555

Commander
Pacific Missile Test Center
Geophysics Division
ATTN: Code 3250 (Terry E. Battalino)
Point Mugu, CA 93042-5000

Lockheed Missiles & Space Co., Inc.
Kenneth R. Hardy
Org/91-01 B/255
3251 Hanover Street
Palo Alto, CA 94304-1191

Commander
Naval Ocean Systems Center
ATTN: Code 54 (Dr. Juergen Richter)
San Diego, CA 92152-5000

Meteorologist in Charge
Kwajalein Missile Range
P.O. Box 67
APO San Francisco, CA 96555

U.S. Department of Commerce
Mountain Administration Support
Center
Library, R-51 Technical Reports
325 S. Broadway
Boulder, CO 80303

Dr. Hans J. Liebe
NTIA/ITS S 3
325 S. Broadway
Boulder, CO 80303

NCAR Library Serials
National Center for Atmos Rsch
P.O. Box 3000
Boulder, CO 80307-3000

HQDA
ATTN: DAMI-POI
Washington, D.C. 20310-1067

Mil Asst for Env Sci Ofc of
The Undersecretary of Defense
for Rsch & Engr/R&AT/E&LS
Pentagon - Room 3D129
Washington, D.C. 20301-3080

Director
Naval Research Laboratory
ATTN: Code 4110
Dr. Lothar H. Ruhnke
Washington, D.C. 20375-5000

HQDA
DEAN-RMD/Dr. Gomez
Washington, D.C. 20314

Director
Division of Atmospheric Science
National Science Foundation
ATTN: Dr. Eugene W. Bierly
1800 G. Street, N.W.
Washington, D.C. 20550

Commander
Space & Naval Warfare System Command
ATTN: PMW-145-1G (LT Painter)
Washington, D.C. 20362-5100

Commandant
U.S. Army Infantry
ATTN: ATSH-CD-CS-OR
Dr. E. Dutoit
Fort Benning, GA 30905-5090

USAFETAC/DNE
Scott AFB, IL 62225

Air Weather Service
Technical Library - FL4414
Scott AFB, IL 62225-5458

HQ AWS/DOO
Scott AFB, IL 62225-5008

USAFETAC/DNE
ATTN: Mr. Charles Glauber
Scott AFB, IL 62225-5008

Commander
U.S. Army Combined Arms Combat
ATTN: ATZL-CAW (LTC A. Kyle)
Fort Leavenworth, KS 66027-5300

Commander
U.S. Army Combined Arms Combat
ATTN: ATZL-CDB-A (Mr. Annett)
Fort Leavenworth, KS 66027-5300

Commander
U.S. Army Space Institute
ATTN: ATZI-SI (Maj Koepsell)
Fort Leavenworth, KS 66027-5300

Commander
U.S. Army Space Institute
ATTN: ATZL-SI-D
Fort Leavenworth, KS 66027-7300

Commander
Phillips Lab
ATTN: PL/LYP (Mr. Chisholm)
Hanscom AFB, MA 01731-5000

Director
Atmospheric Sciences Division
Geophysics Directorate
Phillips Lab
ATTN: Dr. Robert A. McClatchey
Hanscom AFB, MA 01731-5000

Raytheon Company
Dr. Charles M. Sonnenschein
Equipment Division
528 Boston Post Road
Sudbury, MA 01776
Mail Stop 1K9

Director
U.S. Army Materiel Systems
Analysis Activity
ATTN: AMXSY-MP (H. Cohen)
APG, MD 21005-5071

Commander
U.S. Army Chemical Rsch,
Dev & Engr Center
ATTN: SMCCR-OPA (Ronald Pennsyle)
APG, MD 21010-5423

Commander
U.S. Army Chemical Rsch,
Dev & Engr Center
ATTN: SMCCR-RS (Mr. Joseph Vervier)
APG, MD 21010-5423

Commander
U.S. Army Chemical Rsch,
Dev & Engr Center
ATTN: SMCCR-MUC (Mr. A. Van De Wal)
APG, MD 21010-5423

Director
U.S. Army Materiel Systems
Analysis Activity
ATTN: AMXSY-AT (Mr. Fred Campbell)
APG, MD 21005-5071

Director
U.S. Army Materiel Systems
Analysis Activity
ATTN: AMXSY-CR (Robert N. Marchetti)
APG, MD 21005-5071

Director
U.S. Army Materiel Systems
Analysis Activity
ATTN: AMXSY-CS (Mr. Brad W. Bradley)
APG, MD 21005-5071

Commander
U.S. Army Laboratory Command
ATTN: AMSLC-CG
2800 Powder Mill Road
Adelphi, MD 20783-1145

Commander
Headquarters
U.S. Army Laboratory Command
ATTN: AMSLC-CT
2800 Powder Mill Road
Adelphi, MD 20783-1145

Commander
Harry Diamond Laboratories
ATTN: SLCIS-CO
2800 Powder Mill Road
Adelphi, MD 20783-1197

Director
Harry Diamond Laboratories
ATTN: SLCHD-ST-SP
Dr. Z.G. Sztankay
Adelphi, MD 20783-1197

National Security Agency
ATTN: W21 (Dr. Longbothum)
9800 Savage Road
Ft George G. Meade, MD 20755-6000

U. S. Army Space Technology
and Research Office
ATTN: Brenda Brathwaite
5321 Riggs Road
Gaithersburg, MD 20882

OIC-NAVSWC
Technical Library (Code E-232)
Silver Springs, MD 20903-5000

The Environmental Research
Institute of MI
ATTN: IRIA Library
P.O. Box 8618
Ann Arbor, MI 48107-8618

Commander
U.S. Army Research Office
ATTN: DRXRO-GS (Dr. W.A. Flood)
P.O. Box 12211
Research Trianagle Park, NC 27709

Dr. Jerry Davis
North Carolina State University
Department of Marine, Earth, &
Atmospheric Sciences
P.O. Box 8208
Raleigh, NC 27650-8208

Commander
U. S. Army CECRL
ATTN: CECRL-RG (Dr. H. S. Boyne)
Hanover, NH 03755-1290

Commanding Officer
U.S. Army ARDEC
ATTN: SMCAR-IMI-I, Bldg 59
Dover, NJ 07806-5000

U.S. Army Communications-Electronics
Command Center for EW/RSTA
ATTN: AMSEL-RD-EW-SP
Fort Monmouth, NJ 07703-5303

Commander
U.S. Army Communications-Electronics
Command
ATTN: AMSEL-EW-D (File Copy)
Fort Monmouth, NJ 07703-5303

Headquarters
U.S. Army Communications-Electronics
Command
ATTN: AMSEL-EW-MD
Fort Monmouth, NJ 07703-5303

Commander
U.S. Army Satellite Comm Agency
ATTN: DRCPM-SC-3
Fort Monmouth, NJ 07703-5303

Director
EW/RSTA Center
ATTN: AMSEL-EW-DR
Fort Monmouth, NJ 07703-5303

USACECOM
Center for EW/RSTA
ATTN: AMSEL-RD-EW-SP
Fort Monmouth, NJ 07703-5303

6585th TG (AFSC)
ATTN: RX (CPT Stein)
Holloman AFB, NM 88330

Department of the Air Force
OL/A 2nd Weather Squadron (MAC)
Holloman AFB, NM 88330-5000

PL/WE
Kirtland AFB, NM 87118-6008

Director
U.S. Army TRADOC Analysis Command
ATTN: ATRC-WSS-R
White Sands Missile Range, NM 88002

Rome Laboratory
ATTN: Technical Library RL/DOVL
Griffiss AFB, NY 13441-5700

Department of the Air Force
7th Squadron
APO, NY 09403

AWS
USAREUR/AEAWX
APO, NY 09403-5000

AF Wright Aeronautical Laboratories
Avionics Laboratory
ATTN: AFWAL/AARI (Dr. V. Chimelis)
Wright-Patterson AFB, OH 45433

AFMC/DOW
Wright-Patterson AFB, OH 0334-5000

Commander
U.S. Army Field Artillery School
ATTN: ATSF-F-FD (Mr. Gullion)
Fort Sill, OK 73503-5600

Commandant
U.S. Army Field Artillery School
ATTN: ATSF-TSM-TA
Mr. Charles Taylor
Fort Sill, OK 73503-5600

Commander
Naval Air Development Center
ATTN: Al Salik (Code 5012)
Warminister, PA 18974

Commander
U.S. Army Dugway Proving Ground
ATTN: STEDP-MT-DA-M
Mr. Paul Carlson
Dugway, UT 84022

Commander
U.S. Army Dugway Proving Ground
ATTN: STEDP-MT-DA-L
Dugway, UT 84022

Commander
U.S. Army Dugway Proving Ground
ATTN: STEDP-MT-M (Mr. Bowers)
Dugway, UT 84022-5000

Defense Technical Information Center
ATTN: DTIC-FDAC
Cameron Station
Alexandria, VA 22314

Commanding Officer
U.S. Army Foreign Science &
Technology Center
ATTN: CM
220 7th Street, NE
Charlottesville, VA 22901-5396

Naval Surface Weapons Center
Code G63
Dahlgren, VA 22448-5000

Commander
U.S. Army OEC
ATTN: CSTE-EFS
Park Center IV
4501 Ford Ave
Alexandria, VA 22302-1458

Commander and Director
U.S. Army Corps of Engineers
Engineer Topographics Laboratory
ATTN: ETL-GS-LB
Fort Belvoir, VA 22060

TAC/DOWP
Langley AFB, VA 23665-5524

U.S. Army Topo Engineering Center
ATTN: CETEC-ZC
Fort Belvoir, VA 22060-5546

Commander
Logistics Center
ATTN: ATCL-CE
Fort Lee, VA 23801-6000

Commander
USATRADOC
ATTN: ATCD-FA
Fort Monroe, VA 23651-5170

Science and Technology
101 Research Drive
Hampton, VA 23666-1340

Commander
U.S. Army Nuclear & Cml Agency
ATTN: MONA-ZB Bldg 2073
Springfield, VA 22150-3198